Chelating N-heterocyclic carbene-carboranes offer flexible ligand coordination to Ir^{III}, Rh^{III} and Ru^{II}: effect of ligand cyclometallation in catalytic transfer hydrogenation

J. Holmes, C. M. Pask and C. E. Willans*

Supporting Information

Table of Contents

Spectroscopic Data

(1-Hydroxyethyl)(2-methyl)-1,2-dicarba-*closo*-dodecaborane

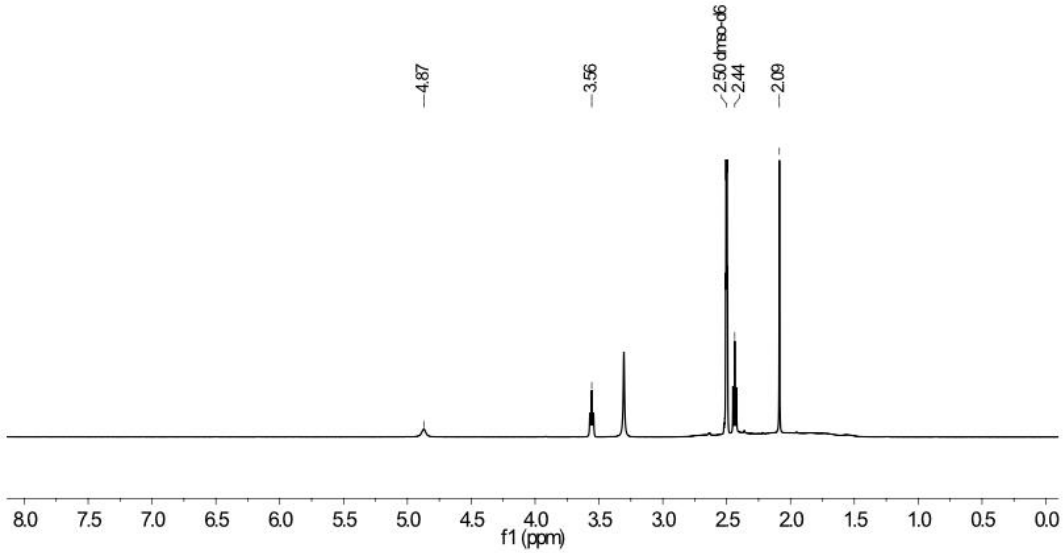

Figure S1. ^{1}H NMR spectrum (dmso-d_6, 500 MHz) of (1-hydroxyethyl)(2-methyl)-1,2-dicarba-*closo*-dodecaborane

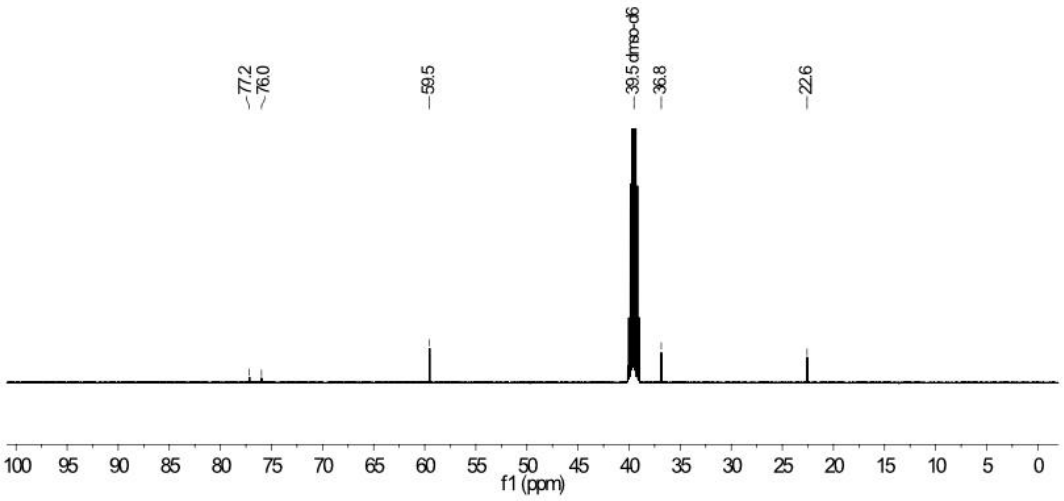

Figure S2. ^{13}C{^{1}H} NMR spectrum (dmso-d_6, 126 MHz) of (1-hydroxyethyl)(2-methyl)-1,2-dicarba-*closo*-dodecaborane

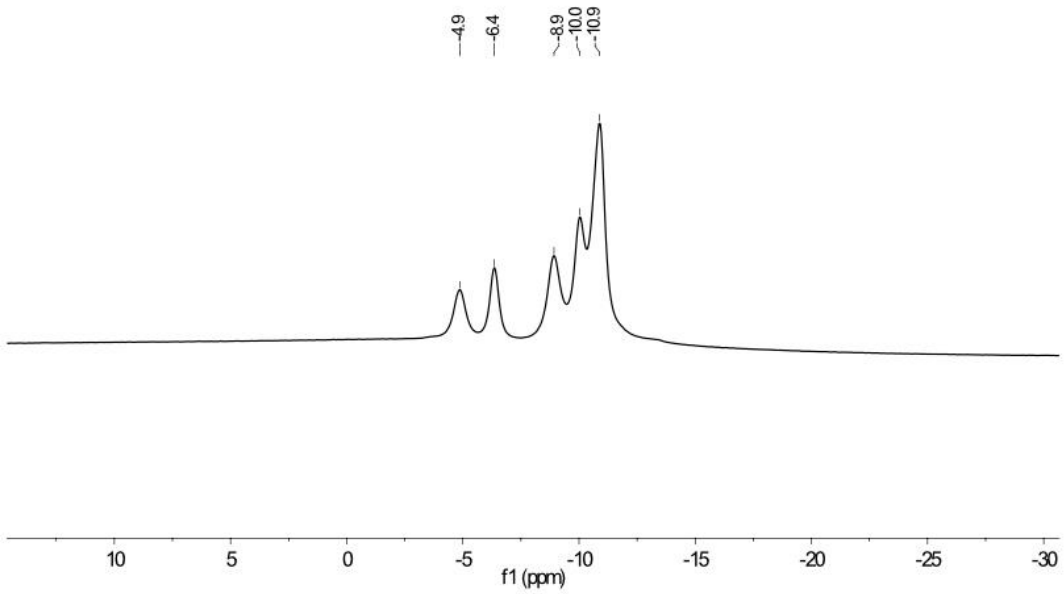

Figure S3. $^{11}B\{^{1}H\}$ NMR spectrum (dmso-d_6, 161 MHz) of (1-hydroxyethyl)(2-methyl)-1,2-dicarba-*closo*-dodecaborane

(1-Bromoethyl)(2-methyl)-1,2-dicarba-*closo*-dodecaborane

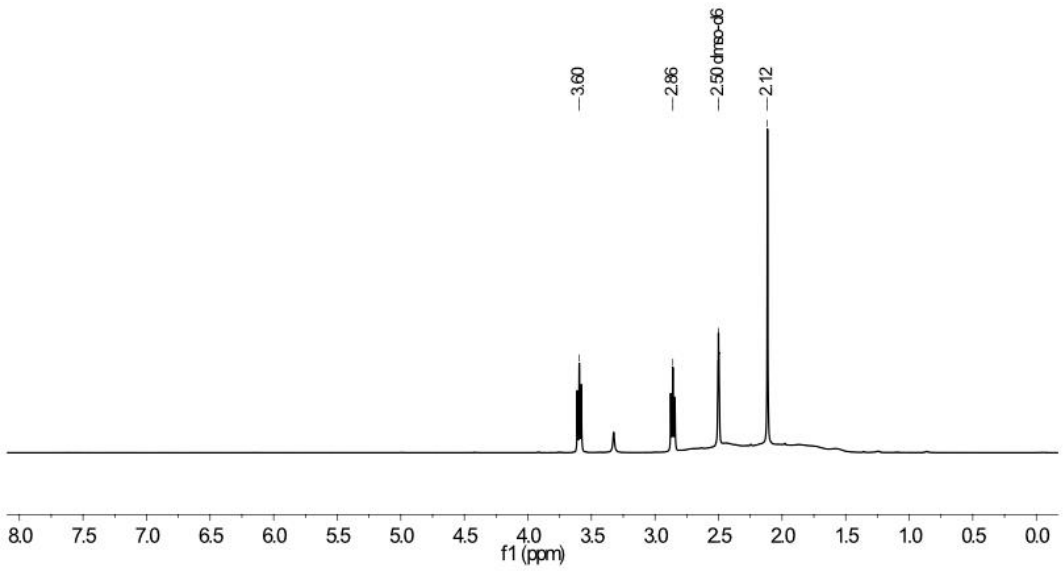

Figure S4. ^{1}H NMR spectrum (dmso-d_6, 500 MHz) of (1-bromoethyl)(2-methyl)-1,2-dicarba-*closo*-dodecaborane

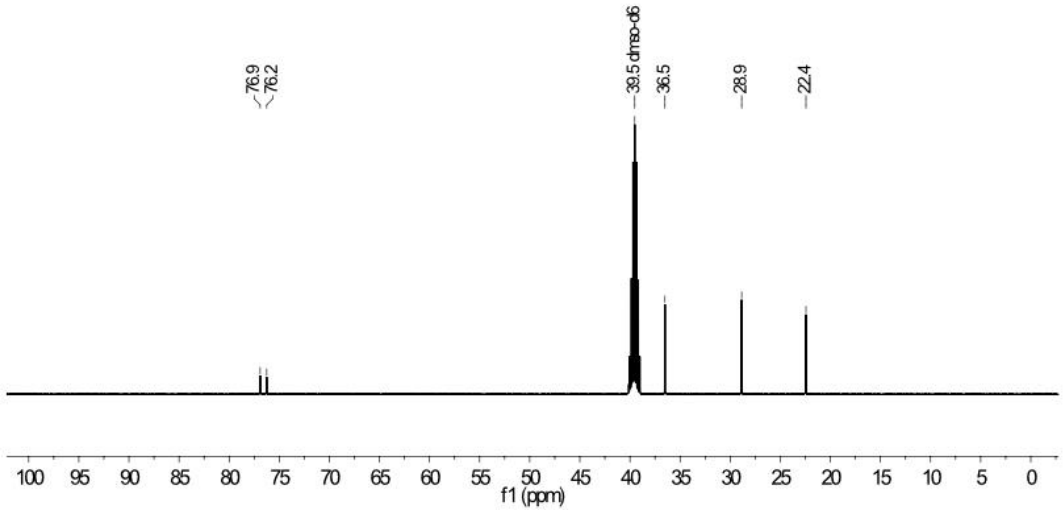

Figure S5. $^{13}C\{^{1}H\}$ NMR spectrum (dmso-d_6, 126 MHz) of (1-bromoethyl)(2-methyl)-1,2-dicarba-*closo*-dodecaborane

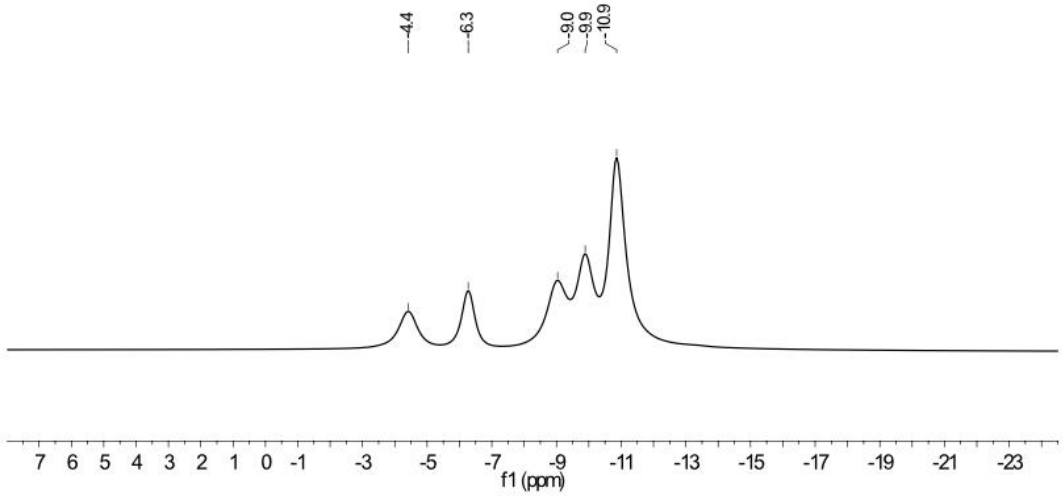

Figure S6. $^{11}B\{^{1}H\}$ NMR spectrum (dmso-d_6, 161 MHz) of (1-bromoethyl)(2-methyl)-1,2-dicarba-*closo*-dodecaborane

Imidazolium bromide salt 1b

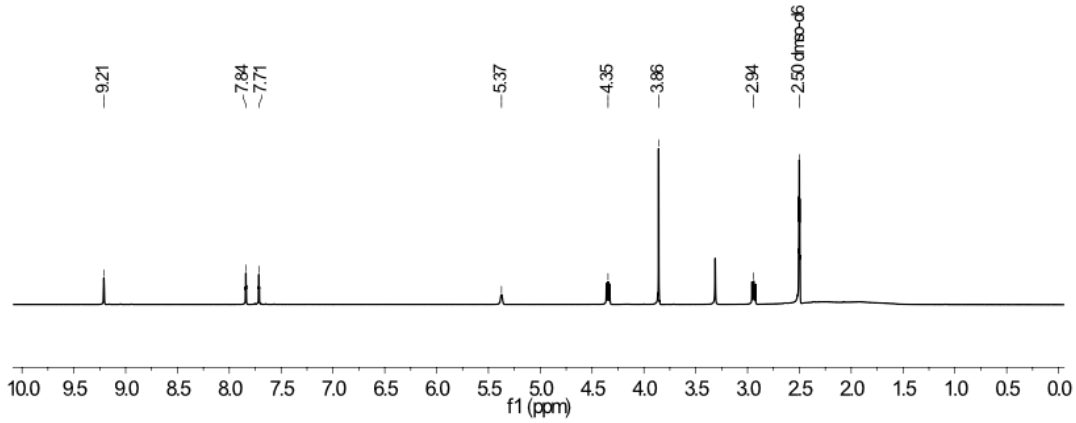

Figure S7. ^{1}H NMR spectrum (dmso-d_6, 500 MHz) of imidazolium bromide salt **1b**

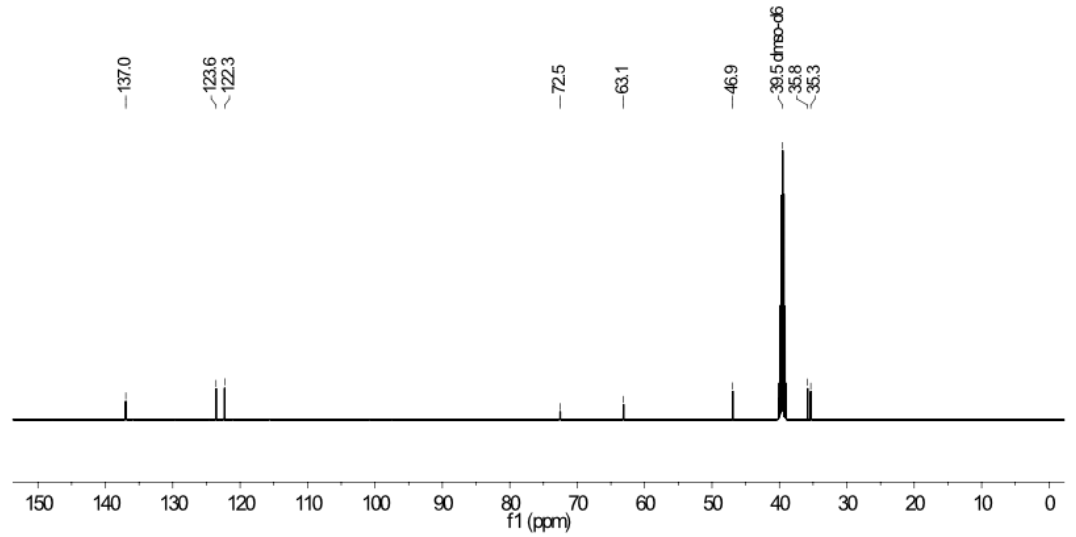

Figure S8. ^{13}C{^{1}H} NMR spectrum (dmso-d_6, 126 MHz) of imidazolium bromide salt **1b**

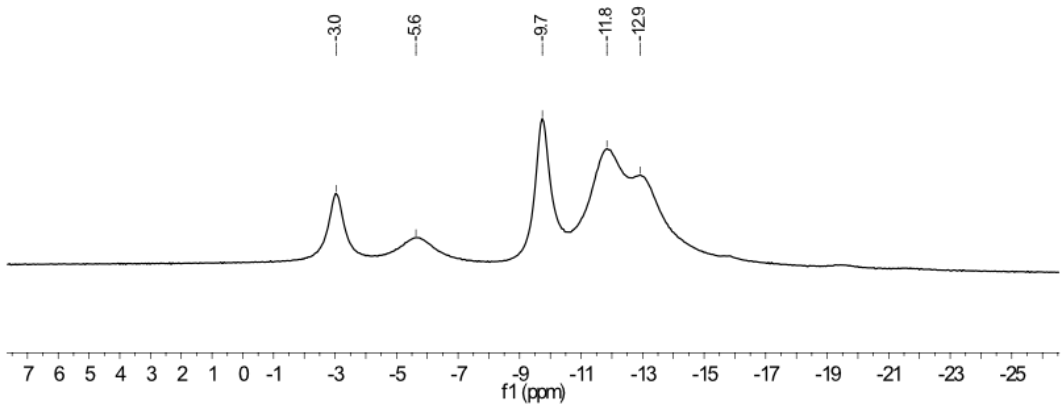

Figure S9. $^{11}B\{^{1}H\}$ NMR spectrum (dmso-d_6, 161 MHz) of imidazolium bromide salt **1b**

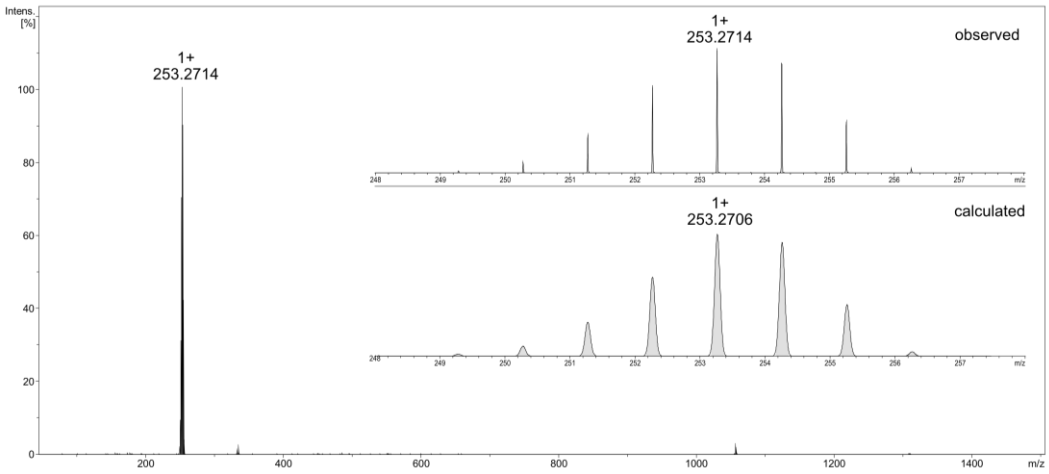

Figure S10. HRMS (ESI^+) of imidazolium salt **1b**

Imidazolium bromide salt 1c

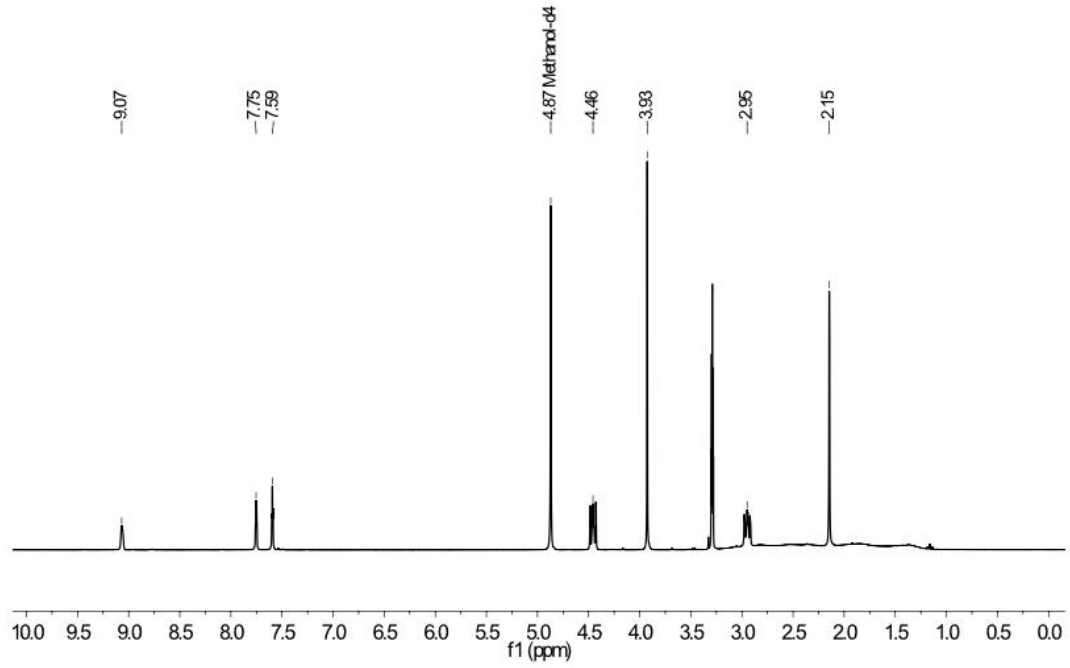

Figure S11. ^{1}H NMR spectrum (CD_3OD, 300 MHz) of imidazolium bromide salt **1c**

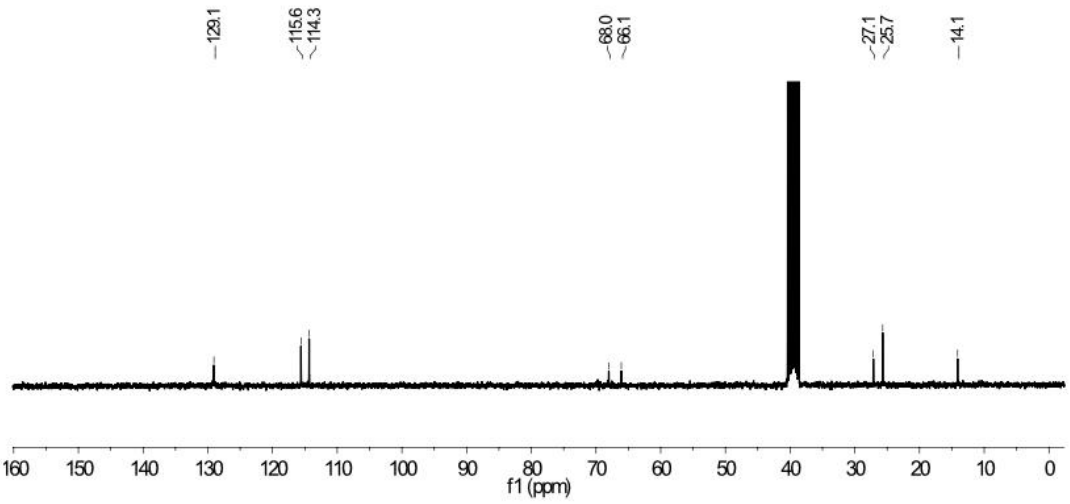

Figure S12. $^{13}C\{^{1}H\}$ NMR spectrum (CD_3OD, 75 MHz) of imidazolium bromide salt **1c**

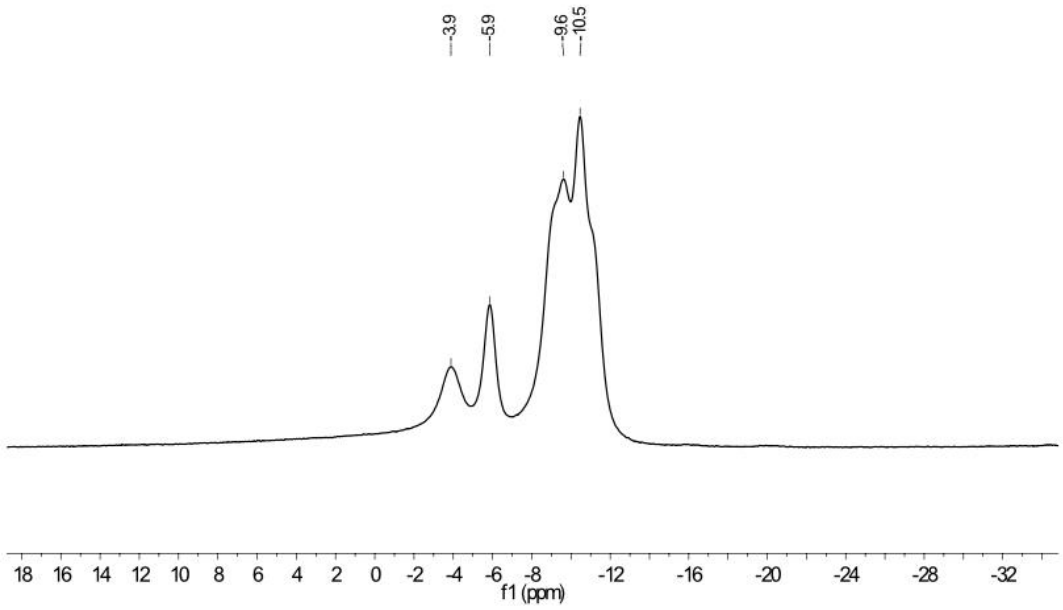

Figure S13. $^{11}B\{^{1}H\}$ NMR spectrum (CD_3OD, 96 MHz) of imidazolium bromide salt **1c**

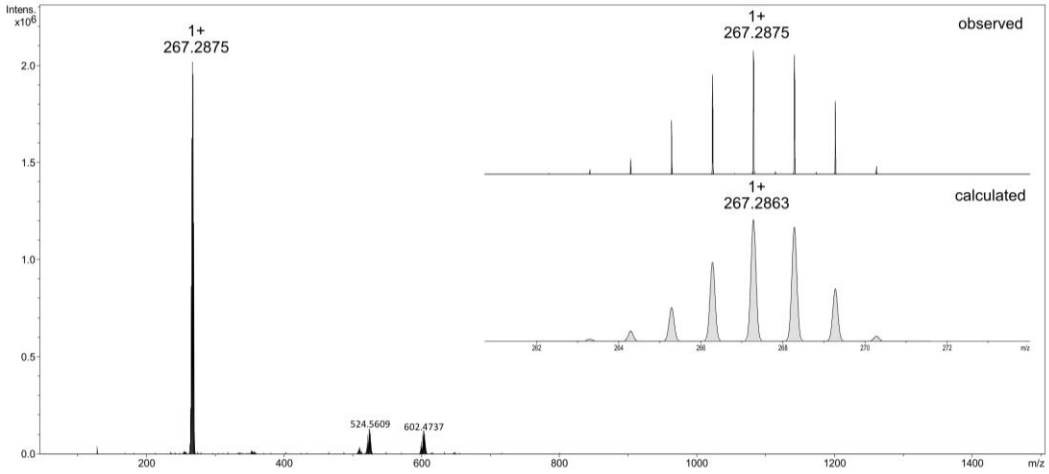

Figure S14. HRMS (ESI^+) of imidazolium salt **1c**.

Ir complex 3a

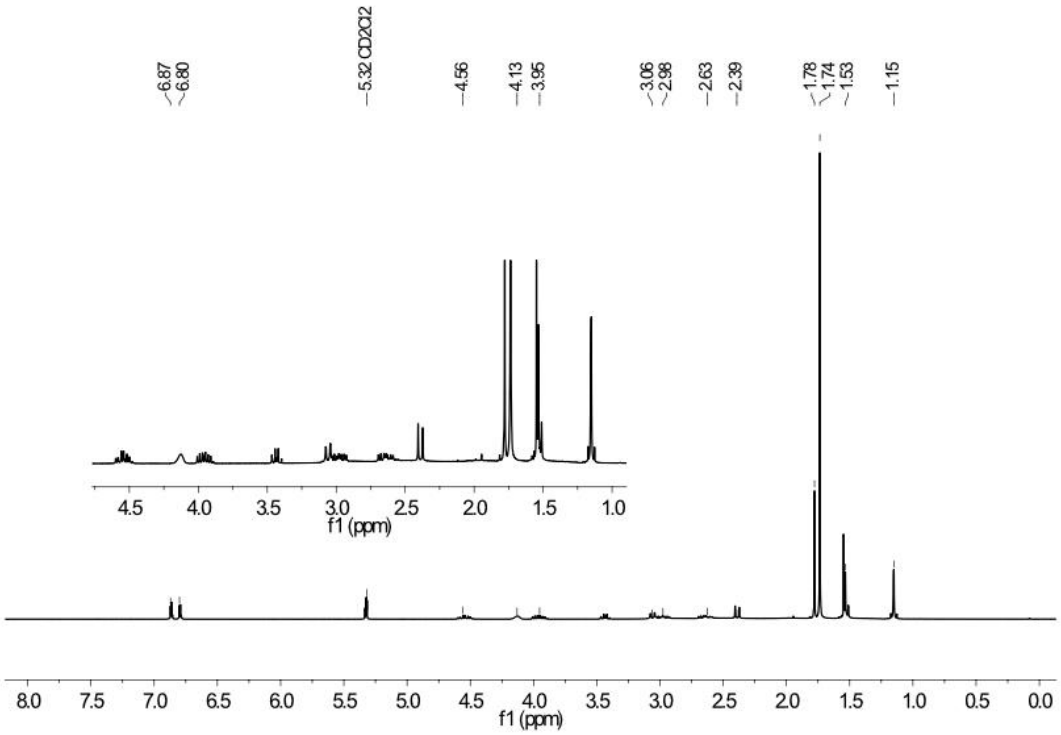

Figure S15. ^{1}H NMR spectrum (CD_2Cl_2, 300 MHz) of complex **3a**

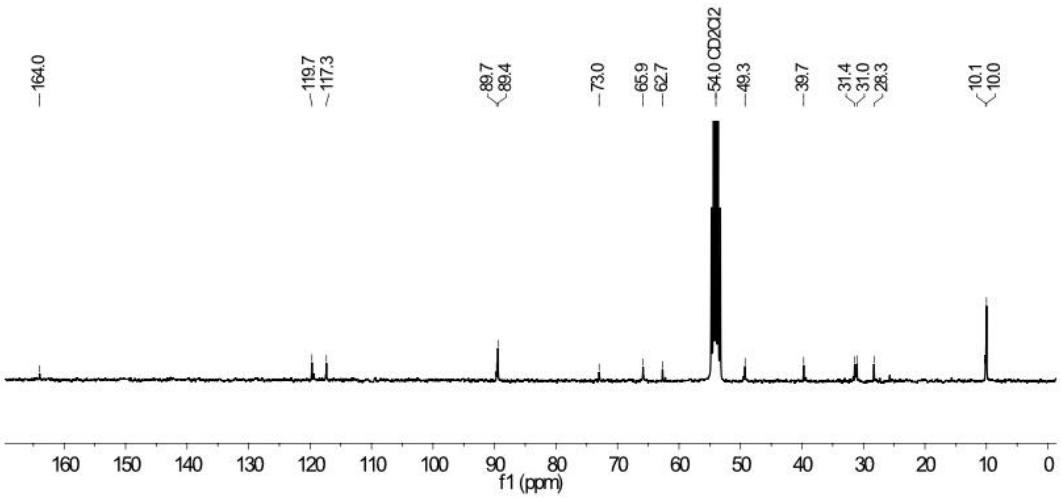

Figure S16. $^{13}C\{^{1}H\}$ NMR spectrum (CD_2Cl_2, 75 MHz) of complex **3a**

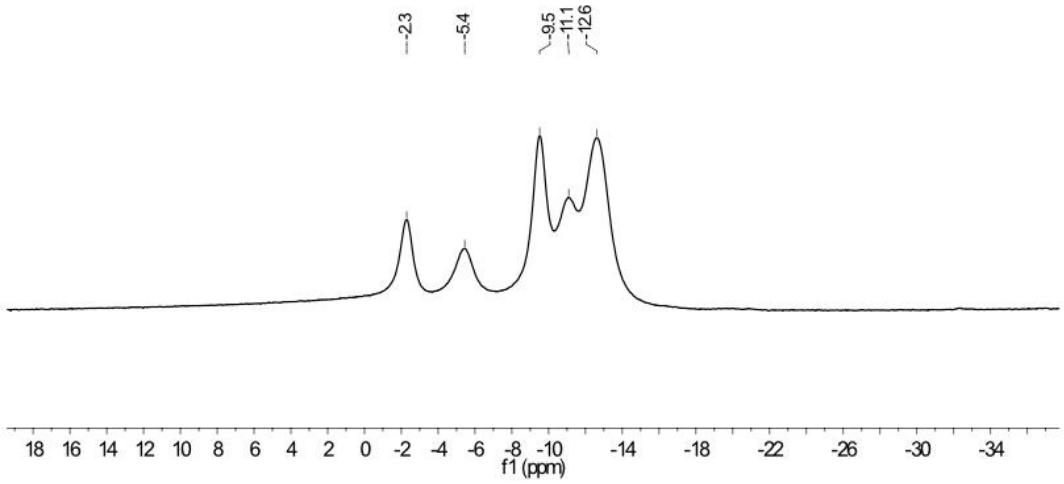

Figure S17. $^{11}B\{^{1}H\}$ NMR spectrum (CD_2Cl_2, 96 MHz) of complex **3a**

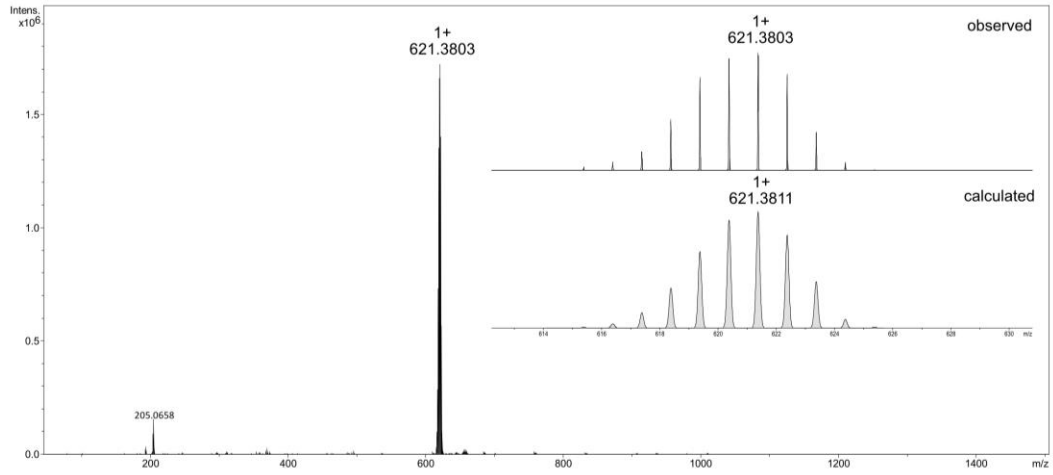

Figure S18. HRMS (ESI^+) of complex **3a**

Ir complex 4a

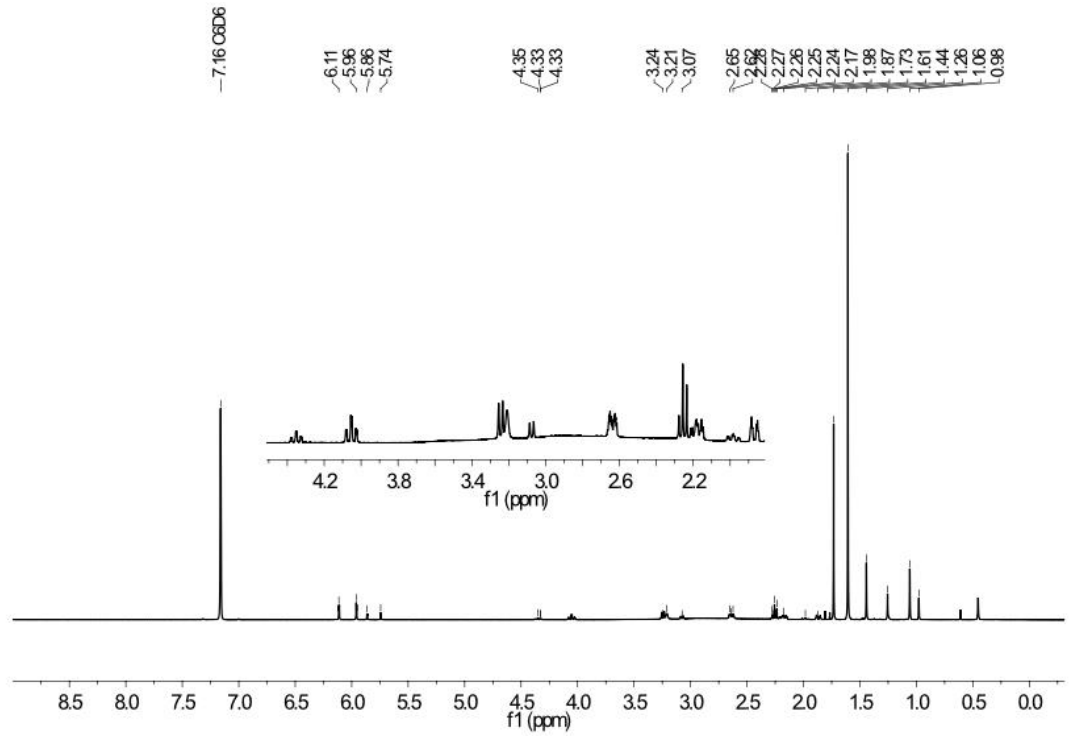

Figure S19. ^{1}H NMR spectrum (C_6D_6, 500 MHz) of complex **4a**

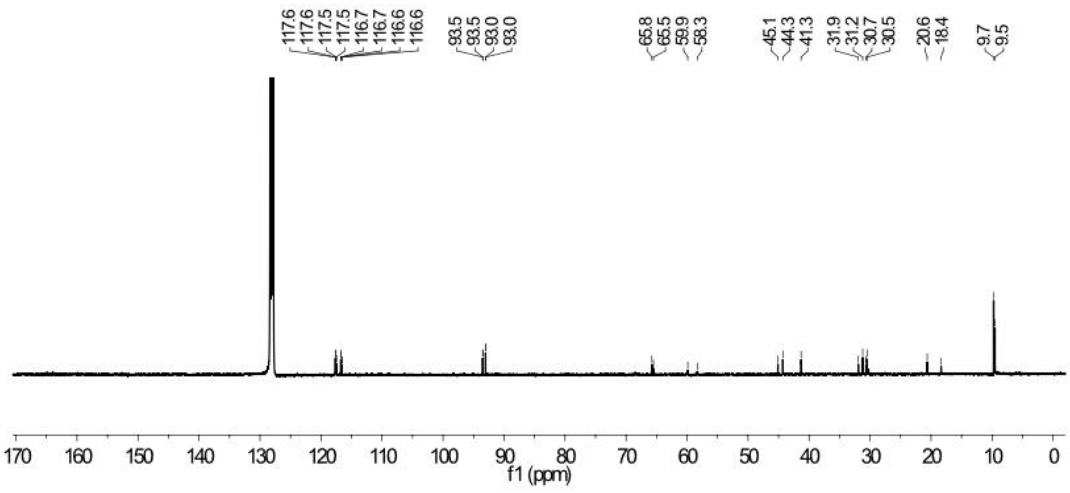

Figure S20. $^{13}C\{^{1}H\}$ NMR spectrum (C_6D_6, 75 MHz) of complex **4a**

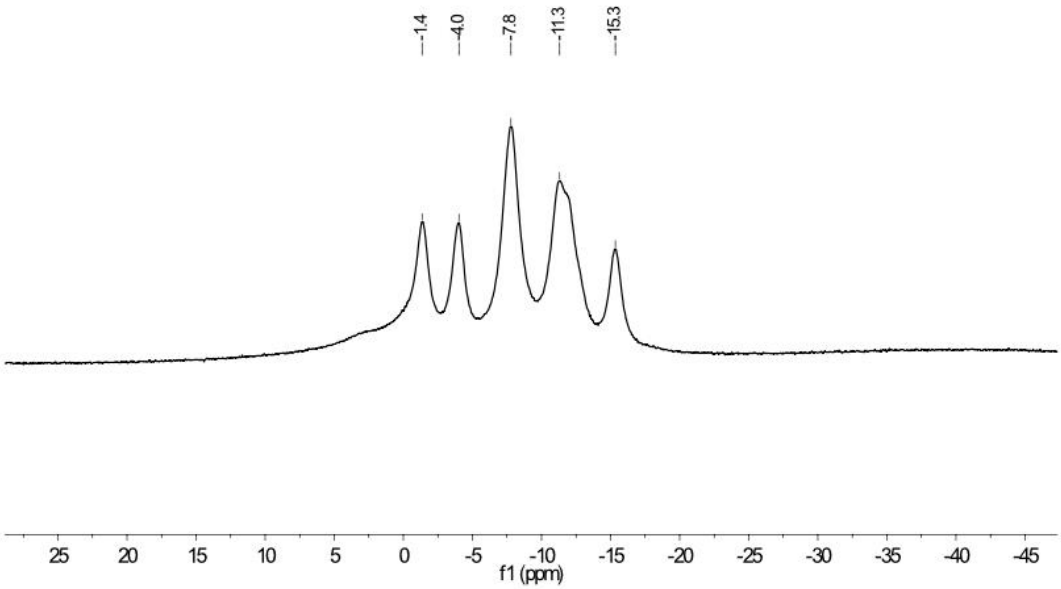

Figure S21. $^{11}B\{^{1}H\}$ NMR spectrum (C_6D_6, 96 MHz) of complex **4a**

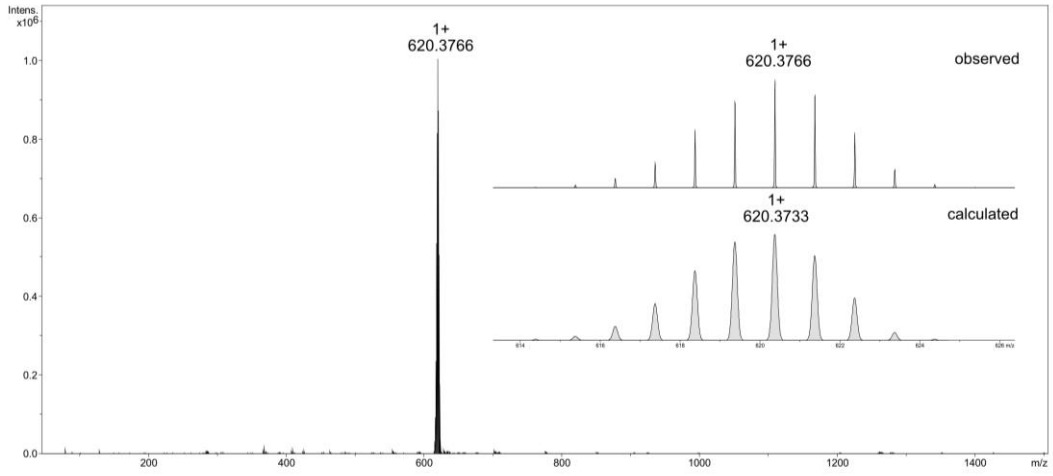

Figure S22. HRMS (ESI^+) of complex **4a**

Ir complex 2b

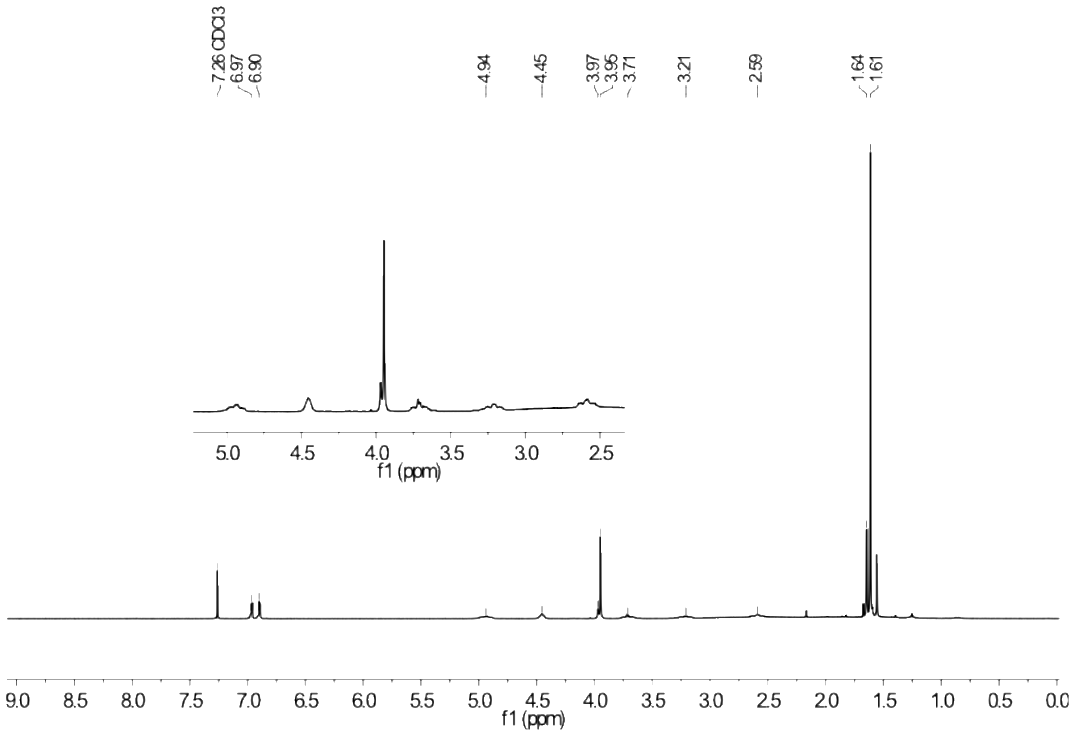

Figure S23. ^{1}H NMR spectrum ($CDCl_3$, 300 MHz) of complex **2b**.

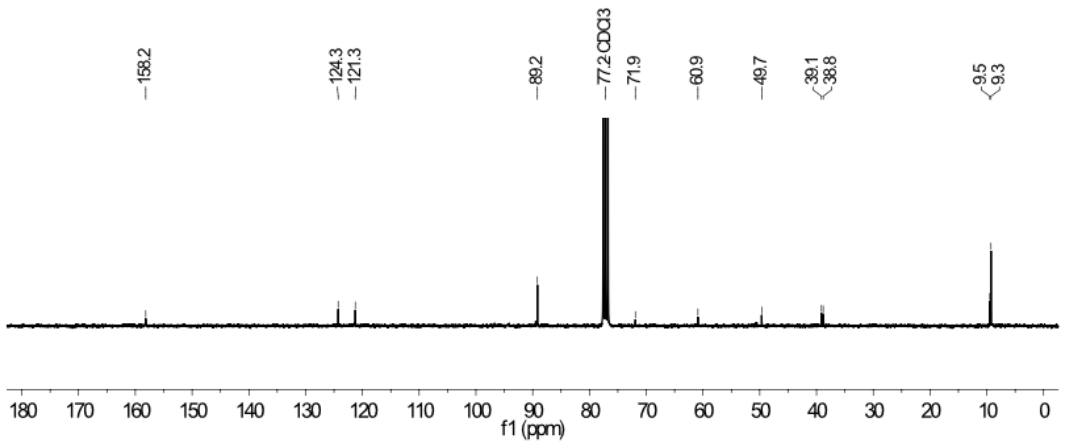

Figure S24. $^{13}C\{^{1}H\}$ NMR spectrum ($CDCl_3$, 75 MHz) of complex **2b**.

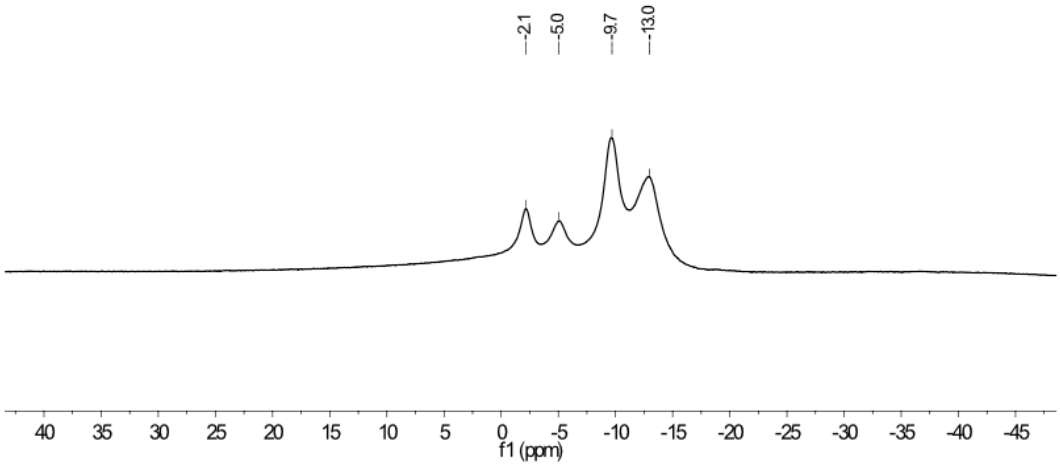

Figure S25. $^{11}B\{^{1}H\}$ NMR spectrum ($CDCl_3$, 96 MHz) of complex **2b**.

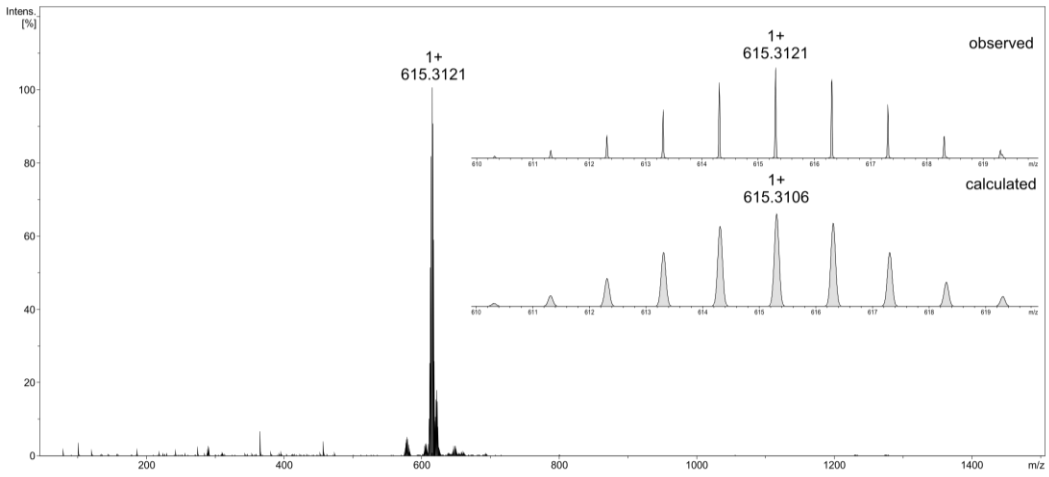

Figure S26. HRMS (ESI^+) of complex **2b**.

Rh complex 5b

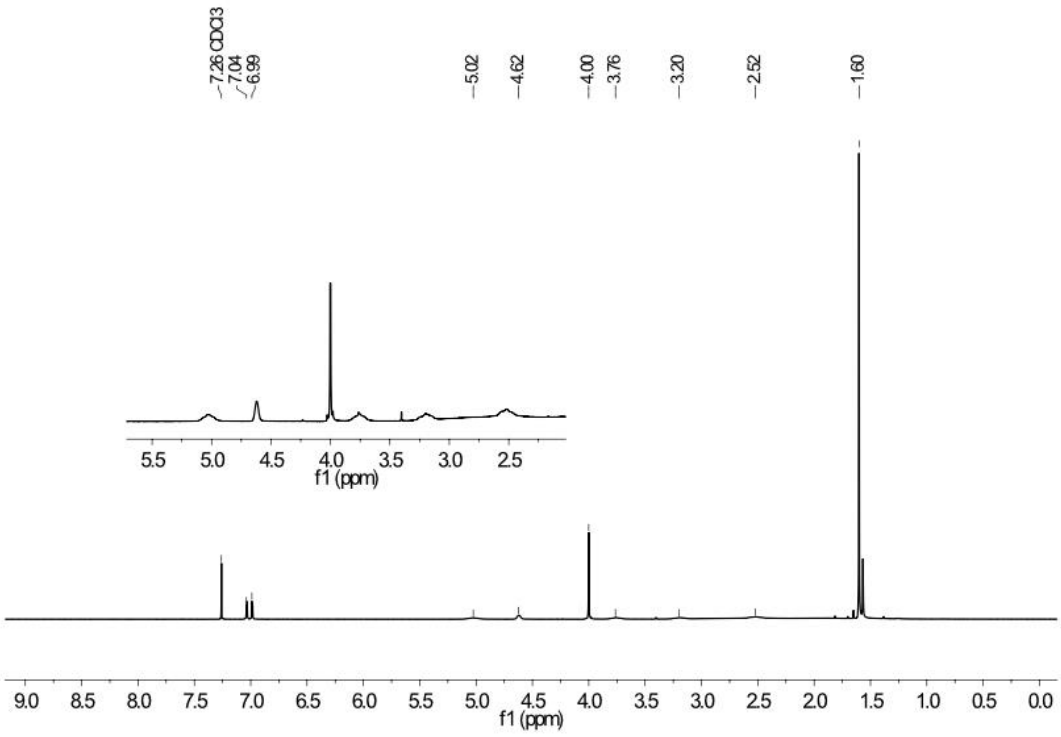

Figure S27. ^{1}H NMR spectrum ($CDCl_3$, 300 MHz) of complex **5b**.

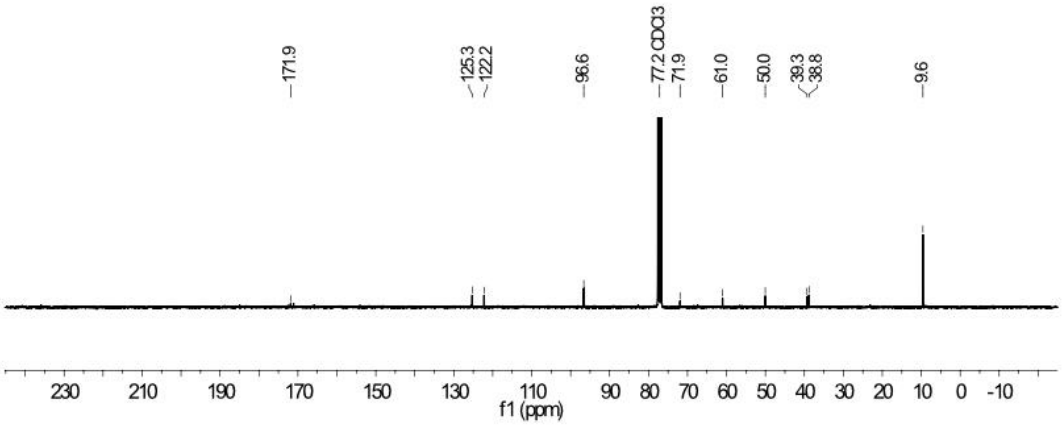

Figure S28. $^{13}C\{^{1}H\}$ NMR spectrum ($CDCl_3$, 75 MHz) of complex **5b**.

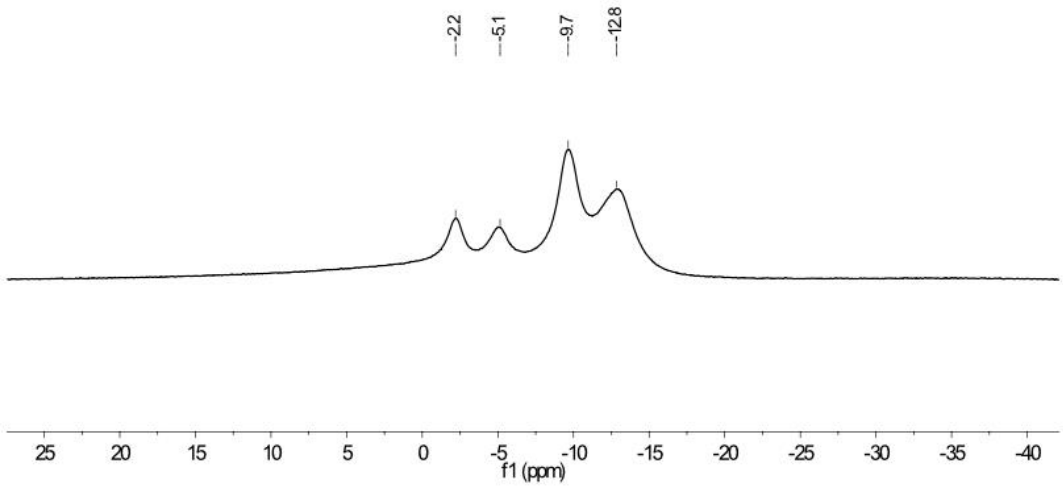

Figure S29. $^{11}B\{^{1}H\}$ NMR spectrum ($CDCl_3$, 96 MHz) of complex **5b**.

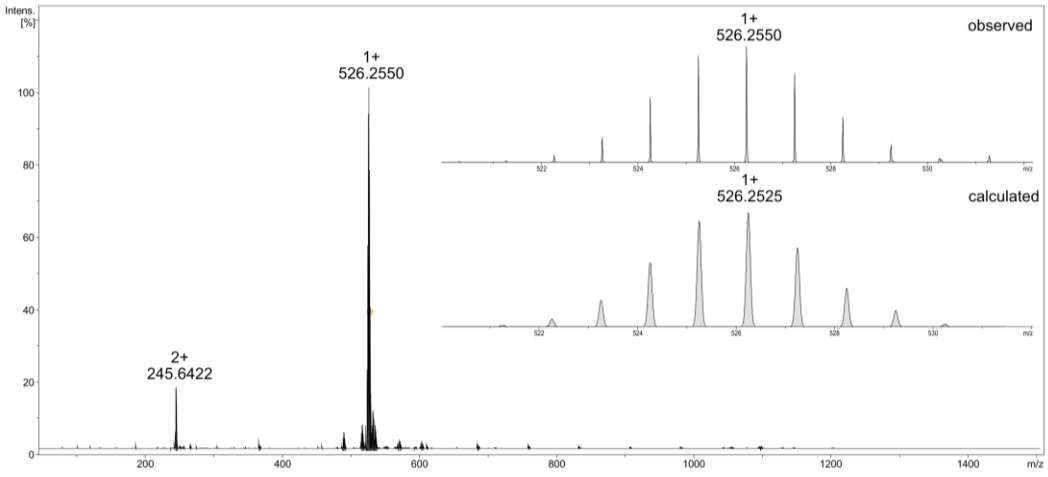

Figure S30. HRMS (ESI^+) of complex **5b**.

Ru complex 6b

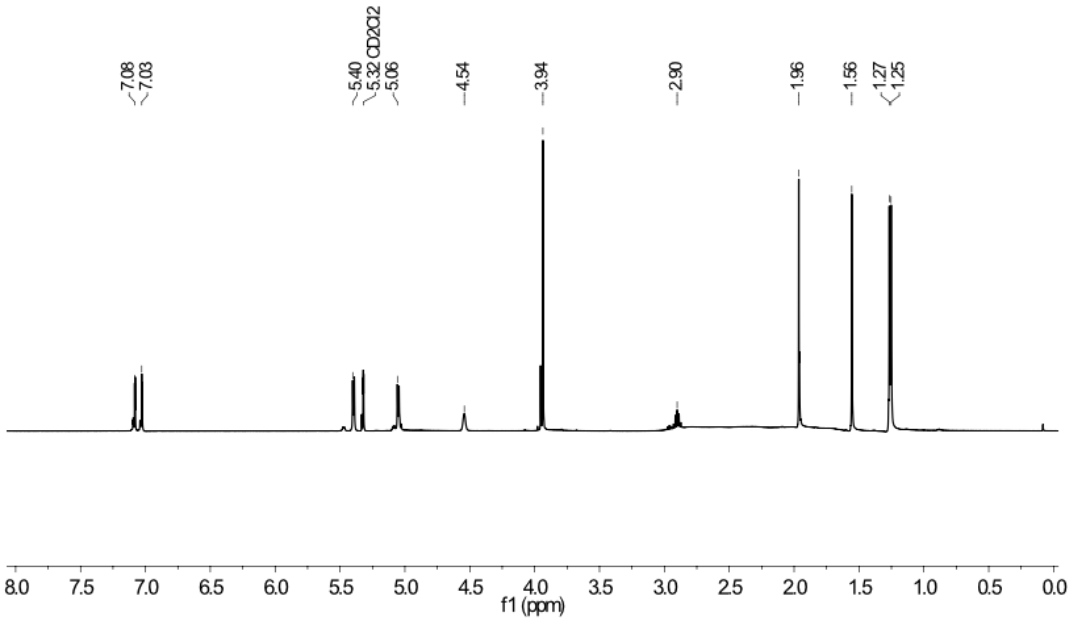

Figure S31. ^{1}H NMR spectrum (CD_2Cl_2, 500 MHz) of complex **6b**.

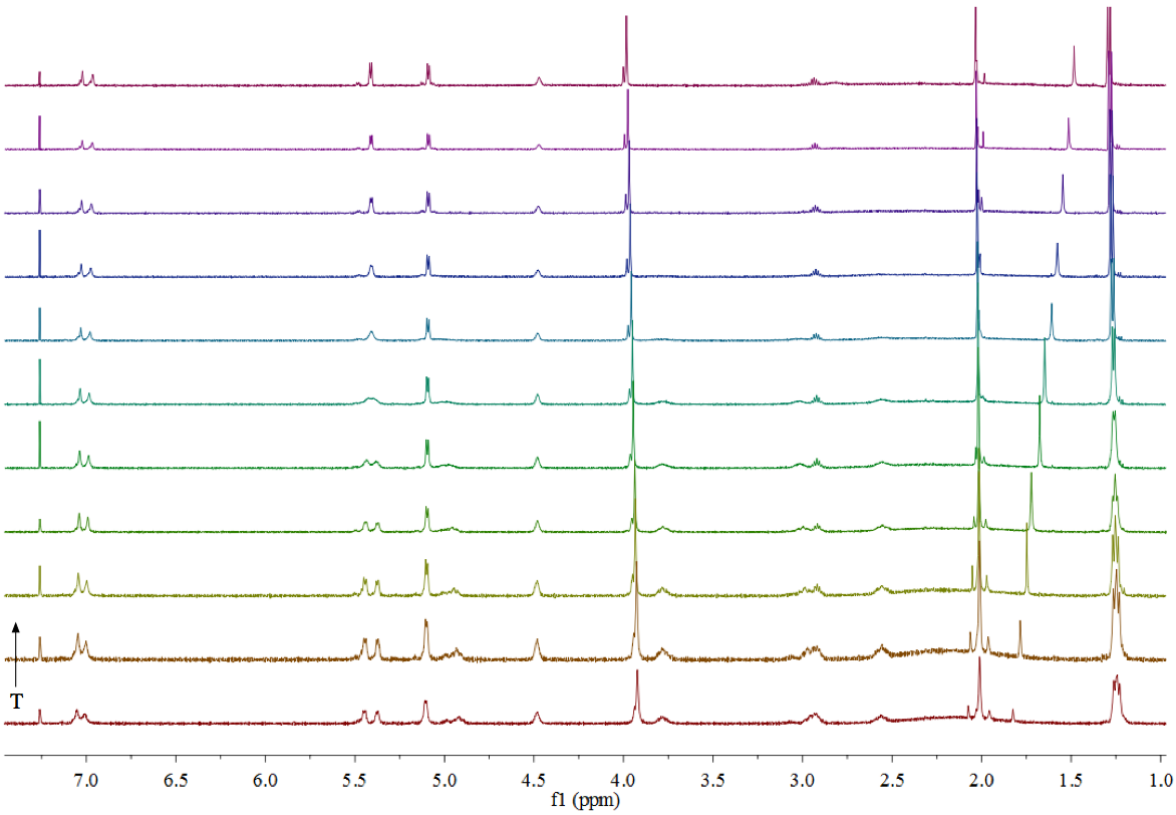

Figure S32. Variable Temperature ^{1}H NMR Spectra (223 K - 323 K, $CDCl_3$) of complex **6b**.

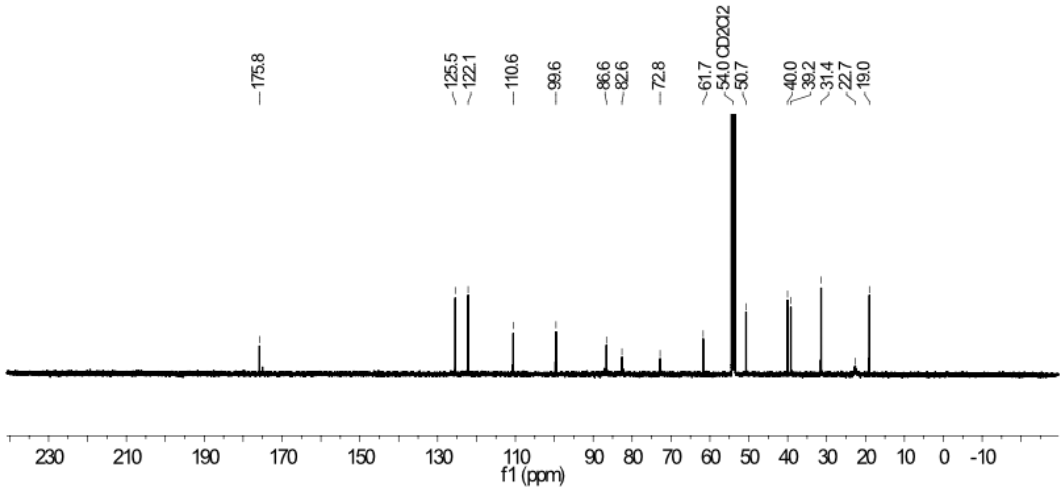

Figure S33. $^{13}C\{^{1}H\}$ NMR spectrum (CD_2Cl_2, 126 MHz) of complex **6b**.

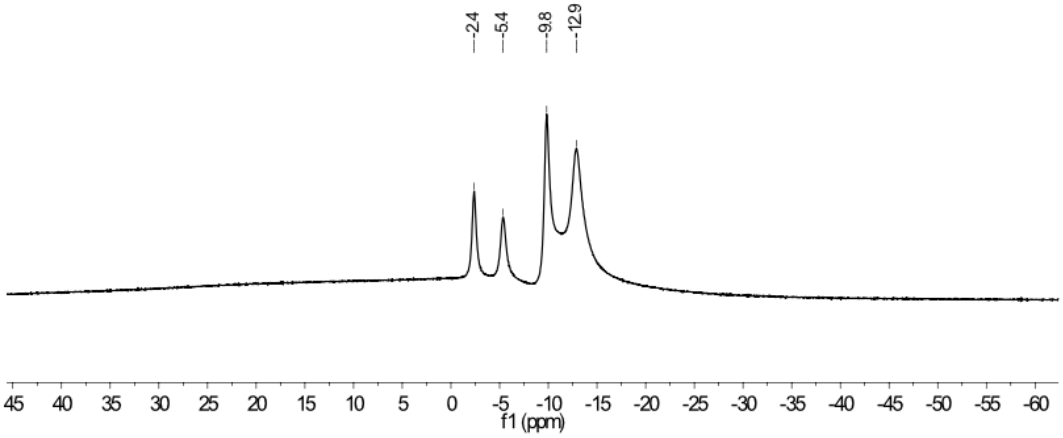

Figure S34. $^{11}B\{^{1}H\}$ NMR spectrum (CD_2Cl_2, 161 MHz) of complex **6b**.

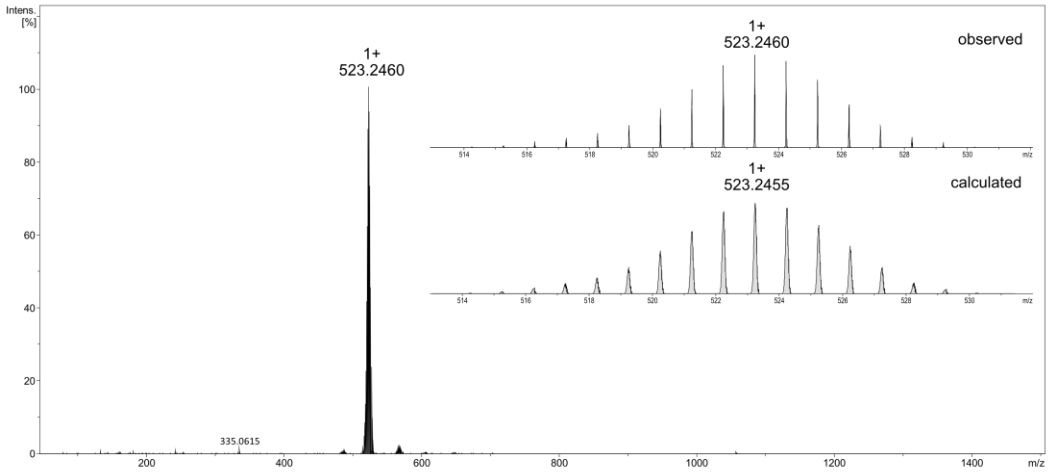

Figure S35. HRMS (ESI$^+$) of complex **6b**.

Mixed Ir complexes 7b/8b

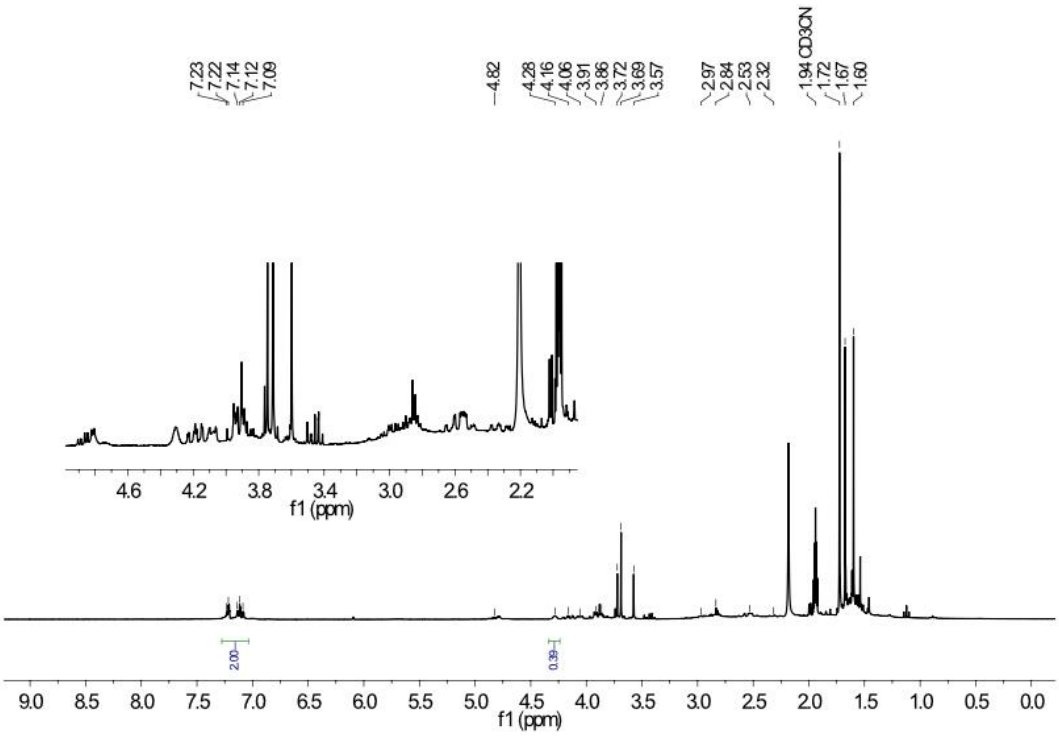

Figure S36. ^{1}H NMR spectrum (CD_2Cl_2, 500 MHz) of complexes **7b** and **8b**.

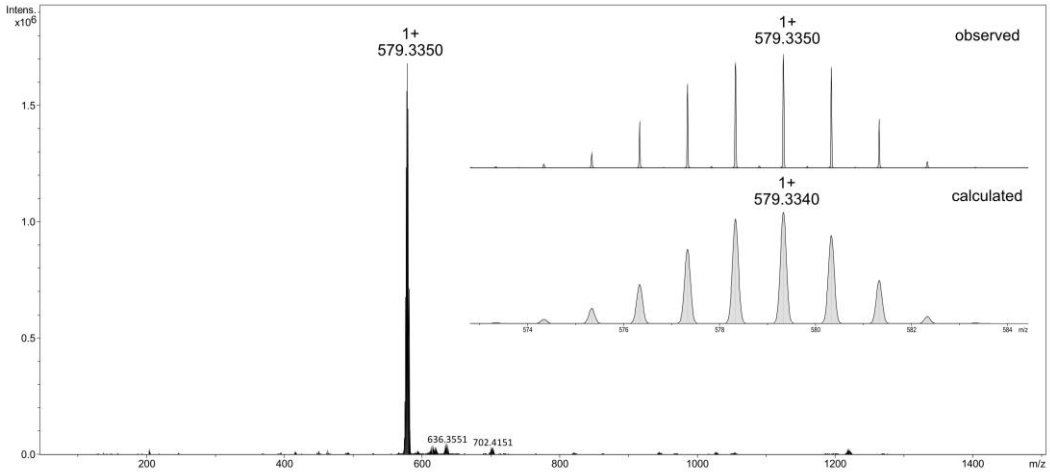

Figure S37. HRMS (ESI^+) of complexes **7b** and **8b**.

Ir complex 7b

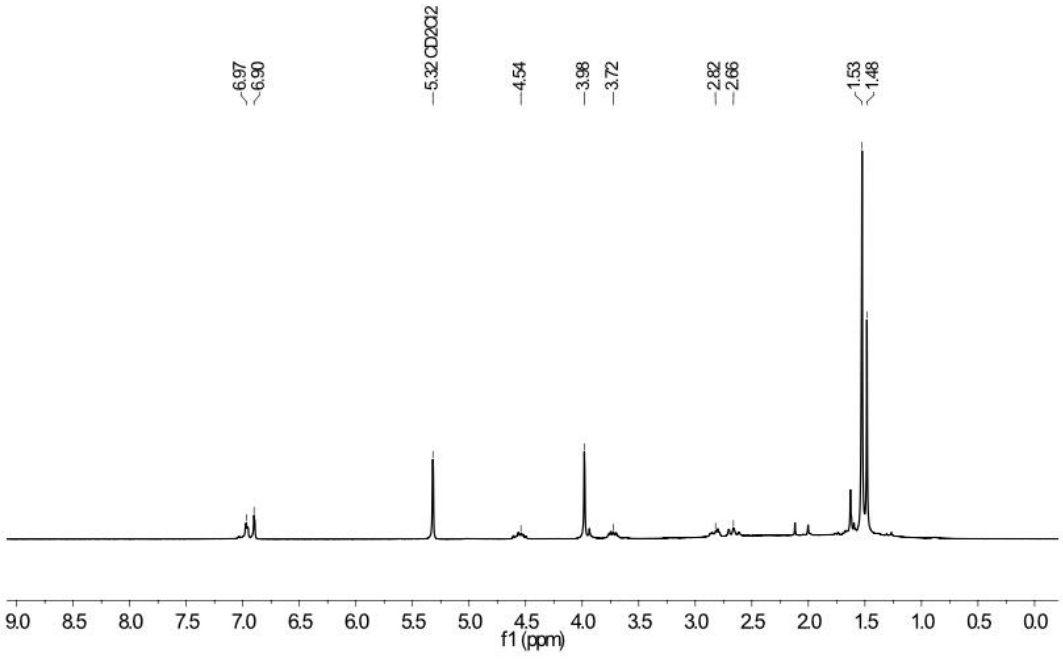

Figure S38. ^1H NMR spectrum (CD_2Cl_2, 300 MHz) of complex **7b**.

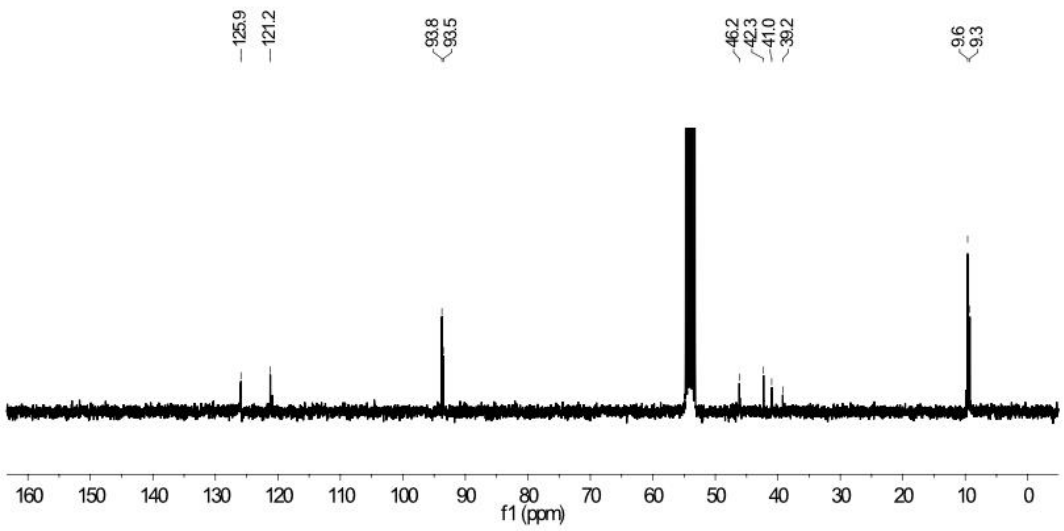

Figure S39. $^{13}C\{^{1}H\}$ NMR spectrum (CD_2Cl_2, 126 MHz) of complex **7b**.

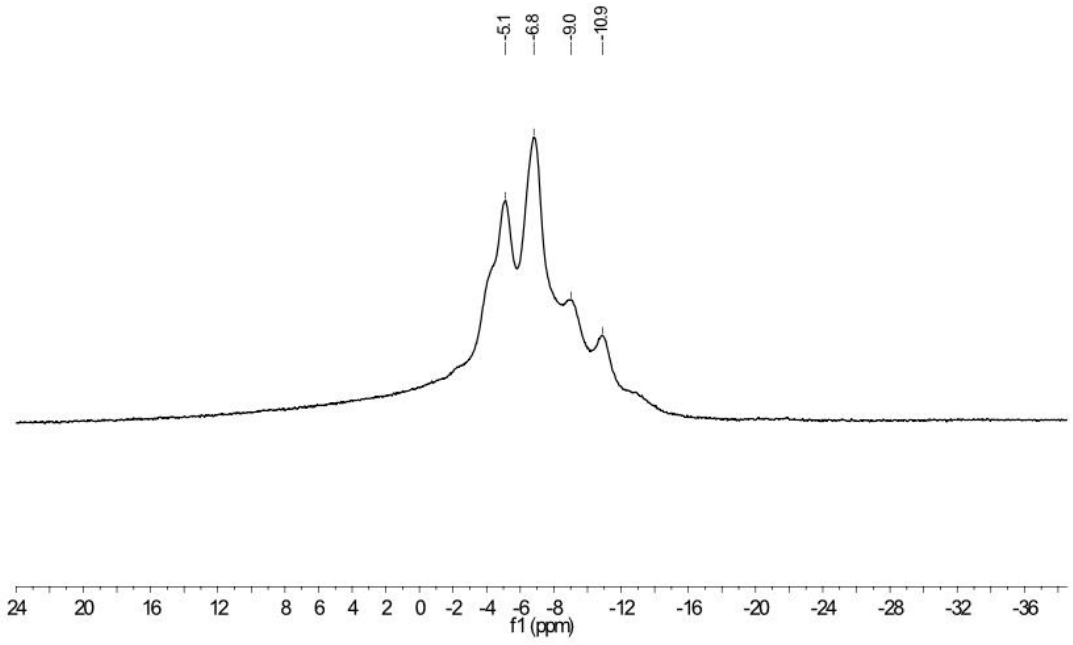

Figure S40. $^{11}B\{^{1}H\}$ NMR spectrum (CD_2Cl_2, 96 MHz) of complex **7b**.

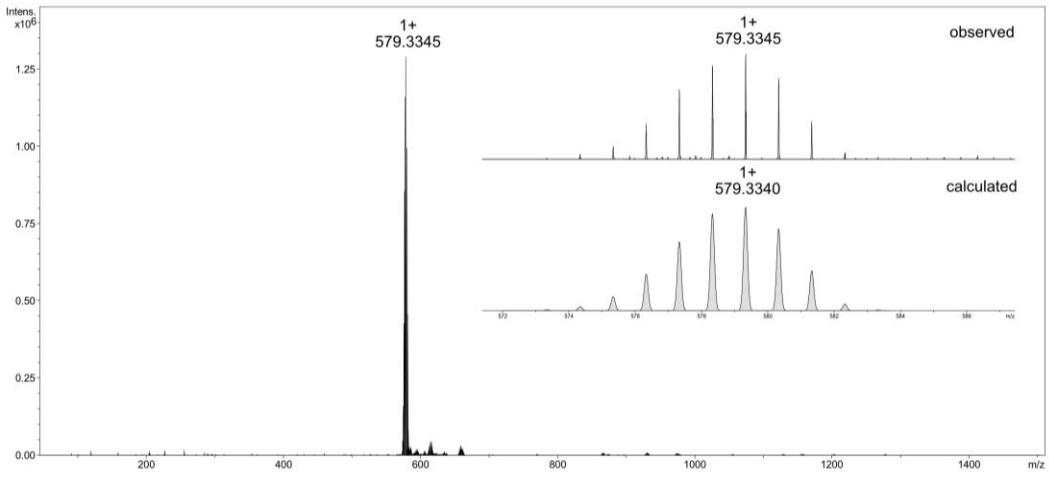

Figure S41. HRMS (ESI^+) of complex **7b**.

Ir complex 2c

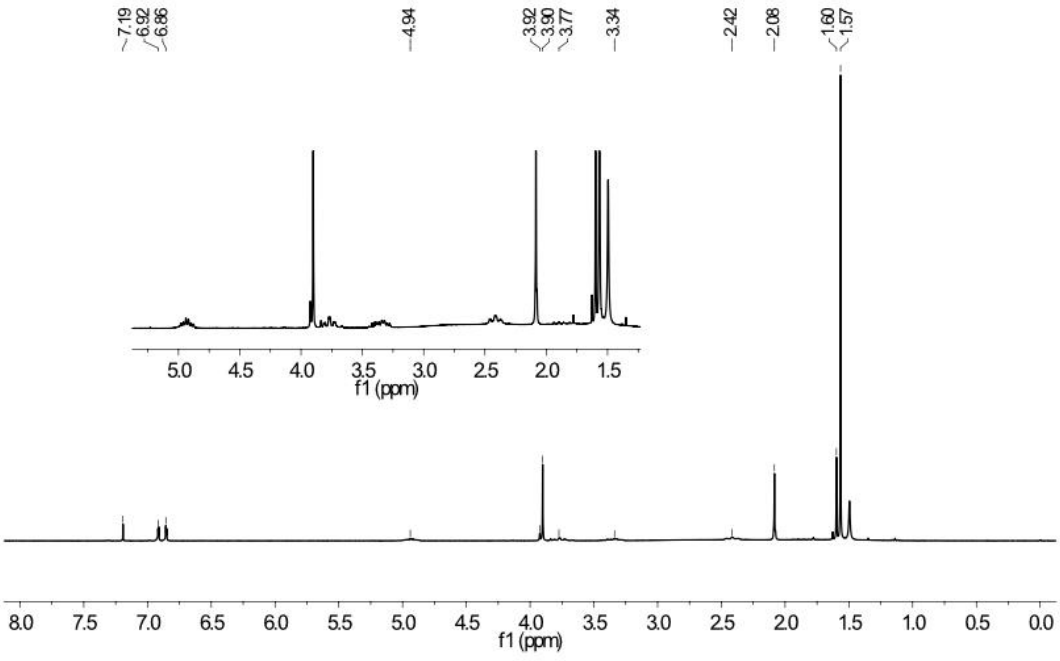

Figure S42. ^1H NMR spectrum ($CDCl_3$, 300 MHz) of complex **2c**.

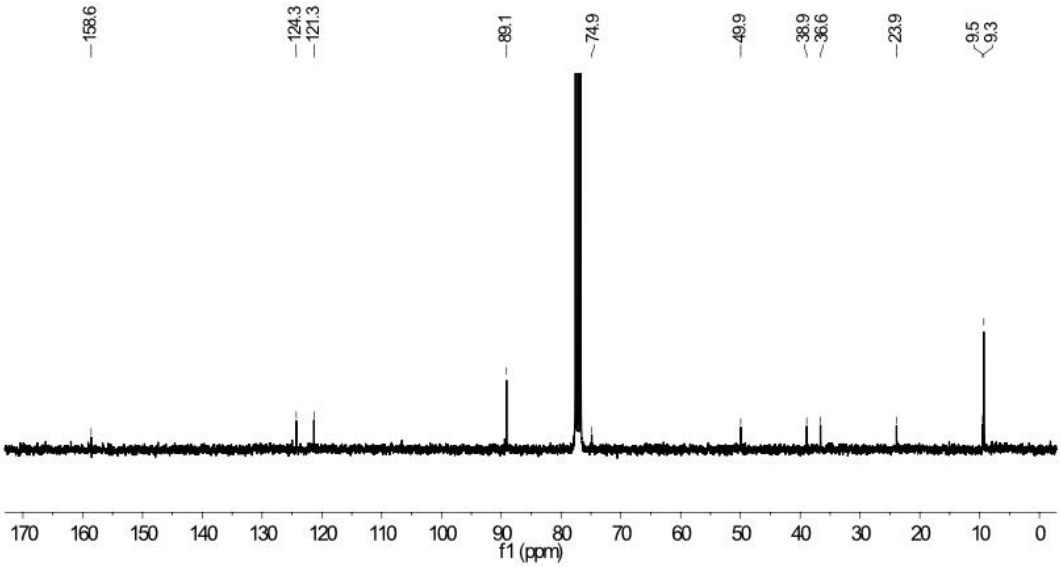

Figure S43. $^{13}C\{^{1}H\}$ NMR spectrum ($CDCl_3$, 75 MHz) of complex **2c**.

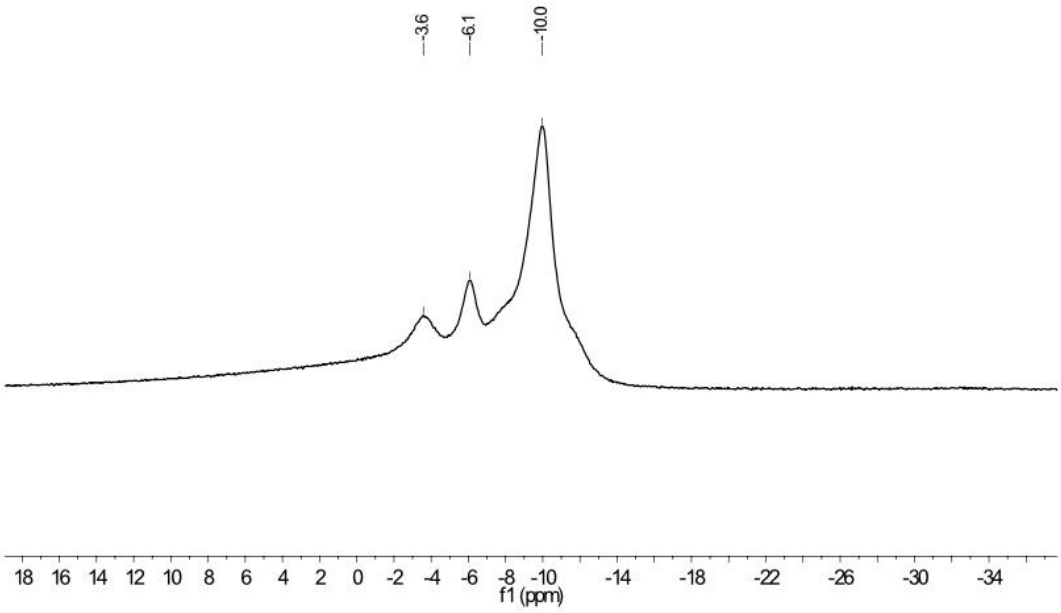

Figure S44. $^{11}B\{^{1}H\}$ NMR spectrum ($CDCl_3$, 96 MHz) of complex **2c**.

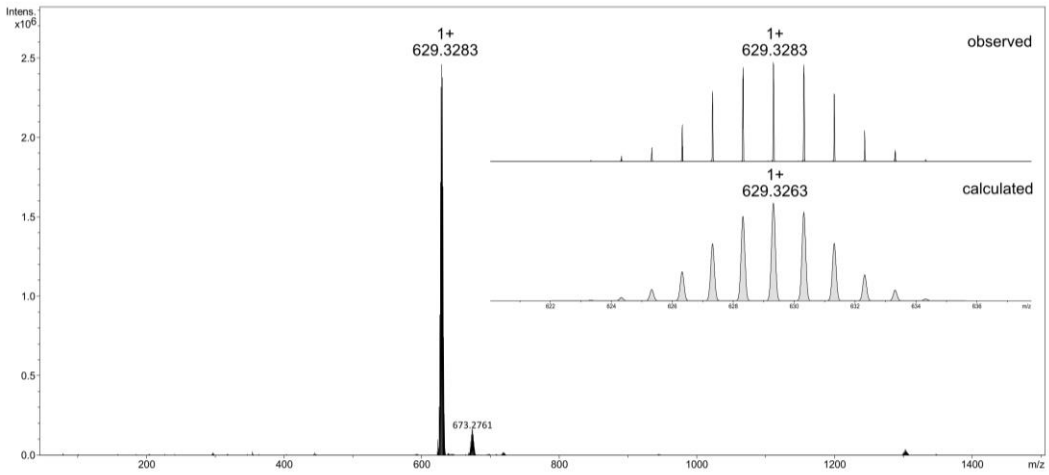

Figure S45. HRMS (ESI$^+$) of complex **2c**.

Ir complex 8c

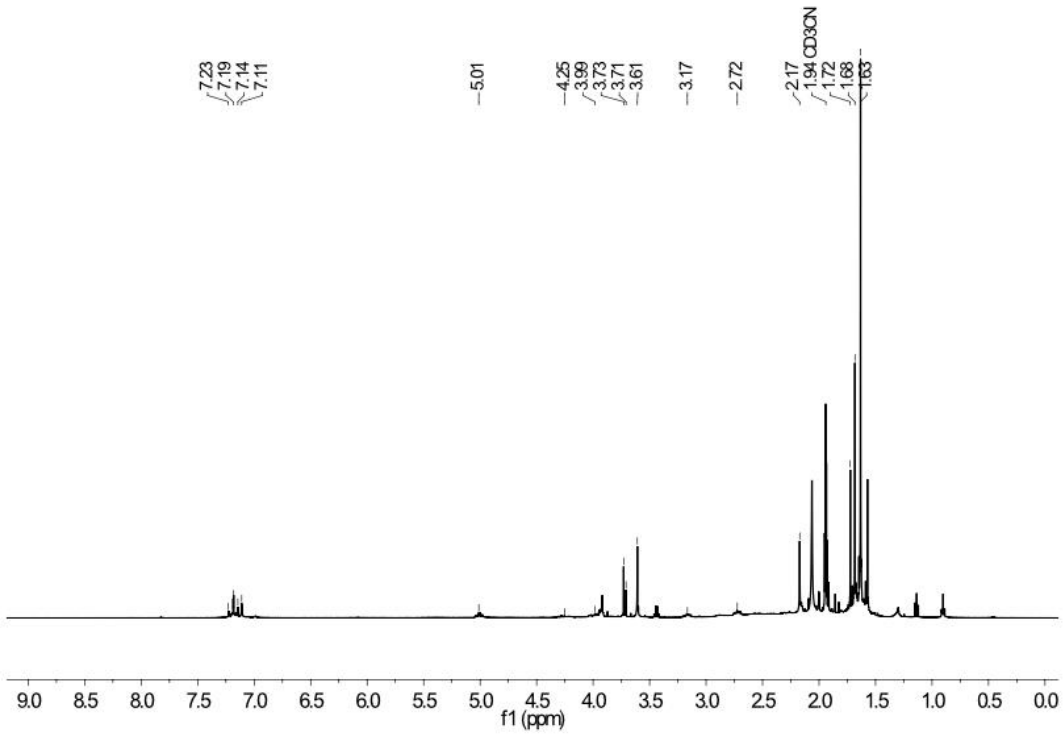

Figure S46. ^{1}H NMR spectrum (CD_3CN, 500 MHz) of complex **8c**.

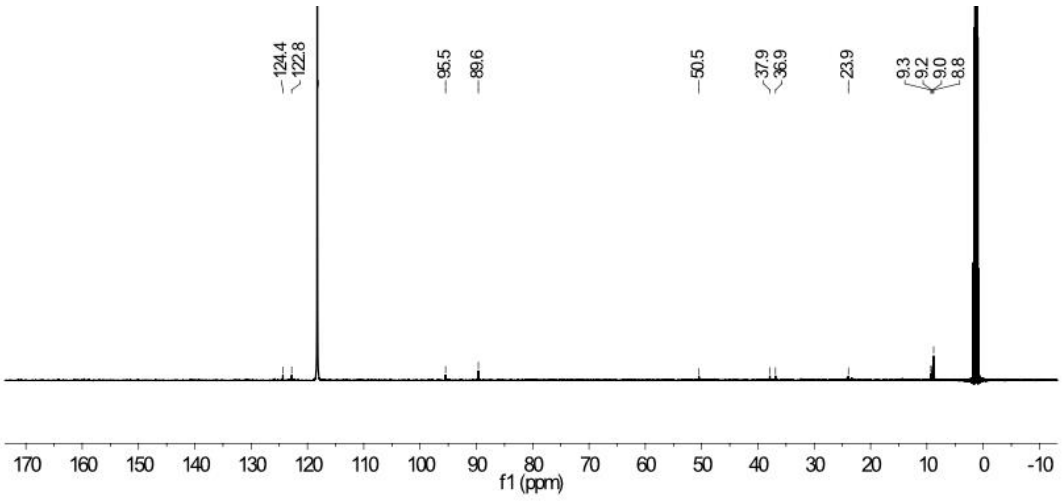

Figure S47. $^{13}C\{^{1}H\}$ NMR spectrum (CD_3CN, 126 MHz) of complex **8c**.

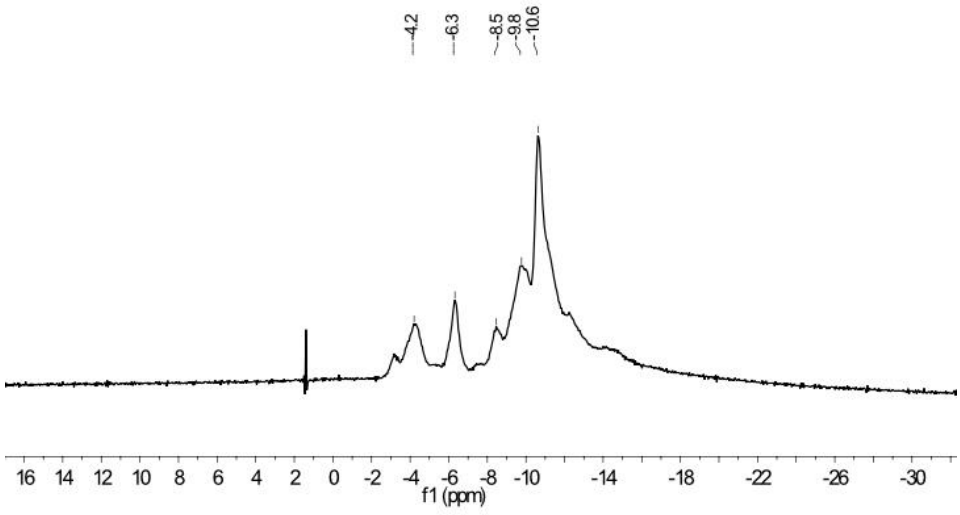

Figure S48. $^{11}B\{^{1}H\}$ NMR spectrum (CD_3CN, 191 MHz) of complex **8c**.

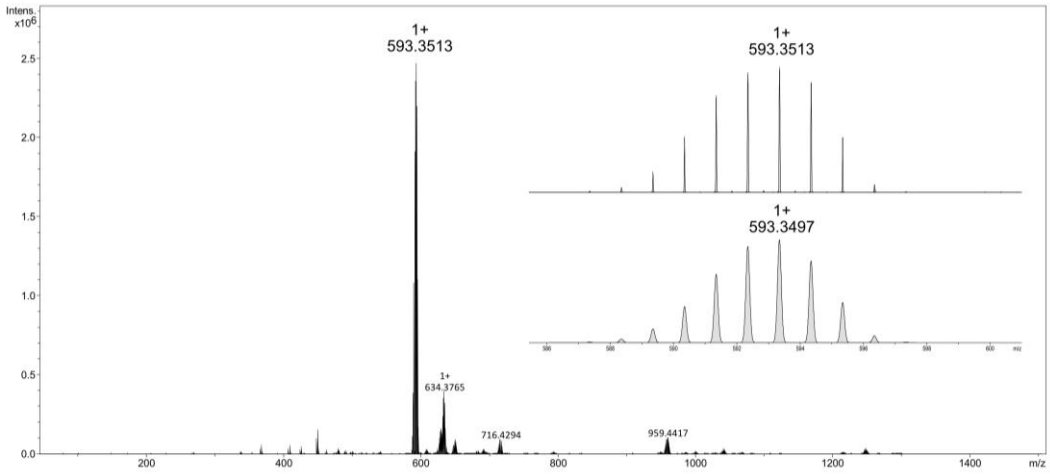

Figure S49. HRMS (ESI^+) of complex **8c**.

Ir complex 2d

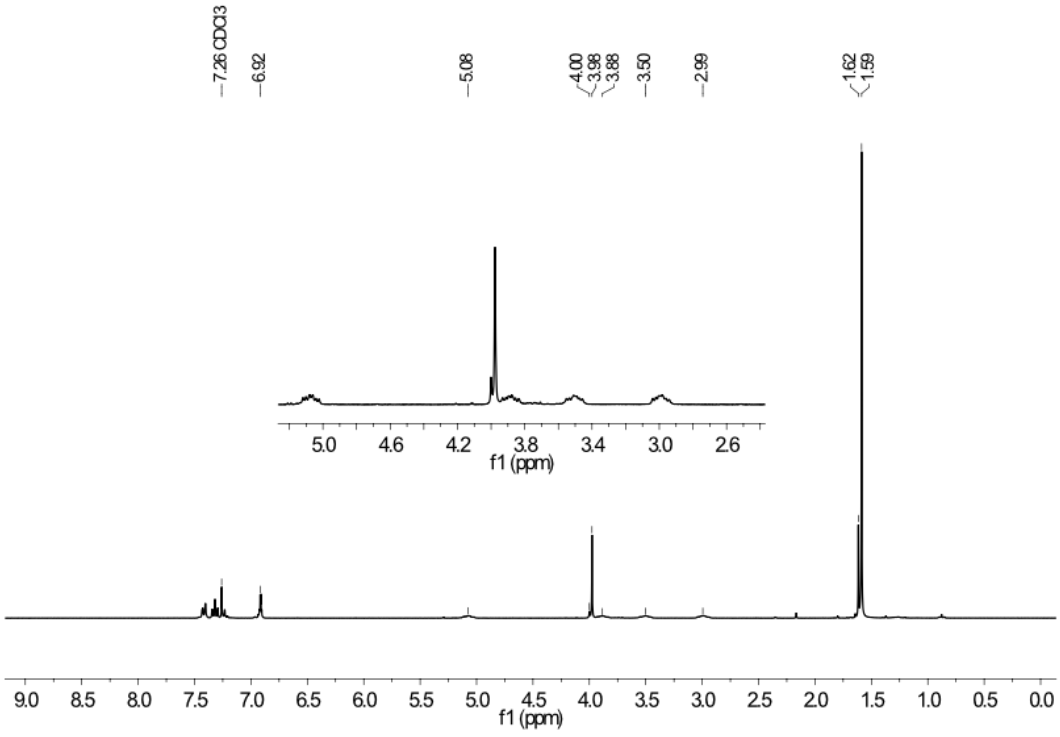

Figure S50. ^1H NMR spectrum ($CDCl_3$, 300 MHz) of complex **2d**.

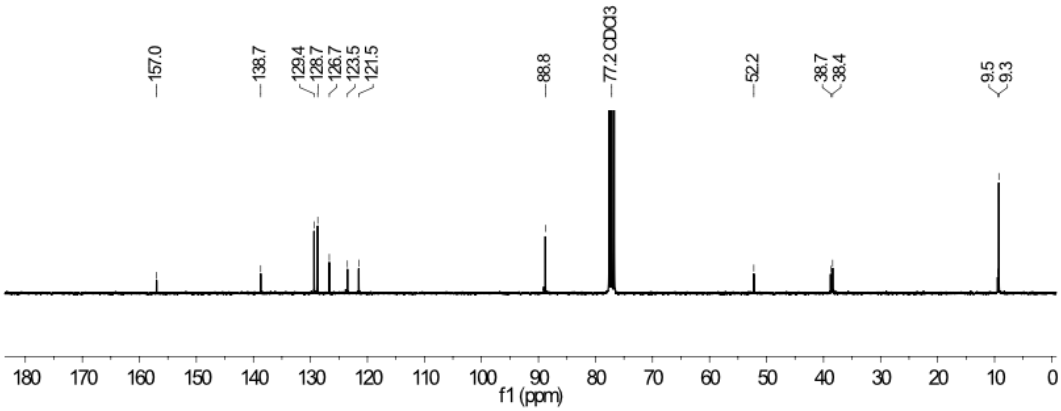

Figure S51. $^{13}C\{^{1}H\}$ NMR spectrum ($CDCl_3$, 75 MHz) of complex **2d**.

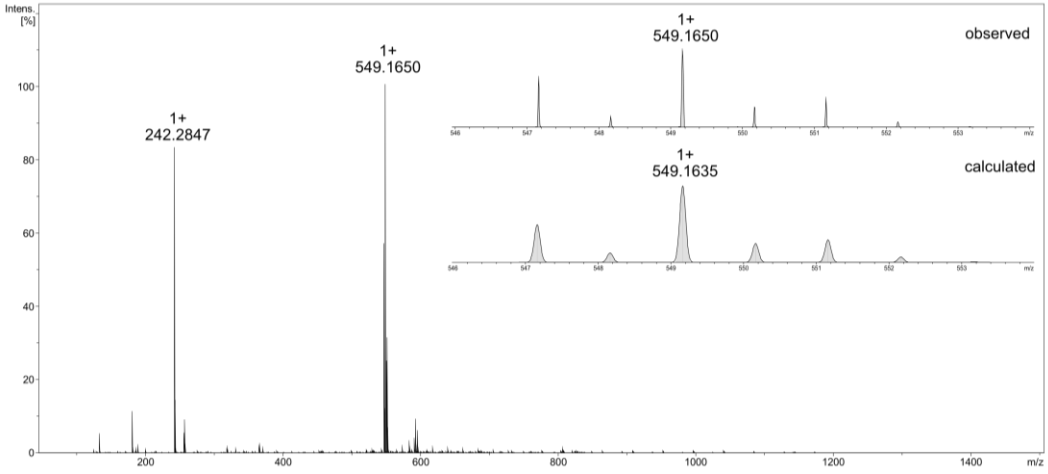

Figure S52. HRMS (ESI^{+}) of complex **2d**.

Crystallographic Data

General Considerations

X-ray diffraction data were collected on an Agilent SuperNova diffractometer fitted with an Atlas CCD detector with Mo- Kα radiation (λ = 0.71073 Å) or Cu- Kα (λ = 1.54184 Å). Crystals were mounted under oil on nylon fibres and data collected at 110, 120 or 293K. Data sets were corrected for absorption using a Gaussian integration method, the structures were solved by direct methods using SHELXS-97[1] or dual-space methods using SHELXT[2] and refined by full-matrix least squares on F^2 using ShelXL-2014,[3] interfaced through the program Olex2.[4] Molecular graphics for all structures were generated using POV-RAY in the X-Seed program.[5,6]

Table S1. Crystal data and structure refinement for imidazolium bromide salt **1b**.

Identification code	1b
Empirical formula	$C_8H_{21}B_{10}BrN_2$
Formula weight	333.28
Temperature/K	110.01(10)
Crystal system	monoclinic
Space group	P2/c
a/Å	12.3901(5)
b/Å	13.1679(5)
c/Å	10.0278(4)
α/°	90
β/°	94.152(4)
γ/°	90
Volume/Å^3	1631.77(11)
Z	4
ρ_{calc}g/cm^3	1.357
μ/mm^{-1}	2.503
F(000)	672.0
Crystal size/mm^3	0.61 × 0.44 × 0.16
Radiation	MoKα (λ = 0.71073)
2Θ range for data collection/°	5.924 to 62.394
Index ranges	-16 ≤ h ≤ 18, -18 ≤ k ≤ 17, -12 ≤ l ≤ 14
Reflections collected	11819
Independent reflections	4614 [R_{int} = 0.0535, R_{sigma} = 0.0703]
Data/restraints/parameters	4614/0/192
Goodness-of-fit on F^2	1.042
Final R indexes [I>=2σ (I)]	R_1 = 0.0461, wR_2 = 0.0965
Final R indexes [all data]	R_1 = 0.0639, wR_2 = 0.1062
Largest diff. peak/hole / e Å^{-3}	0.67/-0.75

Table S2. Crystal data and structure refinement for imidazolium bromide salt **1c**.

Identification code	1c
Empirical formula	$C_9H_{23}B_{10}BrN_2$
Formula weight	347.30
Temperature/K	120.01(15)
Crystal system	orthorhombic
Space group	Pbcn
a/Å	11.9043(3)
b/Å	26.6028(7)
c/Å	10.8820(3)
α/°	90
β/°	90
γ/°	90
Volume/Å^3	3446.19(14)
Z	8
ρ_{calc}g/cm^3	1.339
μ/mm^{-1}	3.107
F(000)	1408.0
Crystal size/mm^3	0.62 × 0.12 × 0.04
Radiation	CuKα (λ = 1.54184)
2Θ range for data collection/°	6.646 to 145.284
Index ranges	-11 ≤ h ≤ 14, -32 ≤ k ≤ 21, -12 ≤ l ≤ 10
Reflections collected	9215
Independent reflections	3313 [R_{int} = 0.0387, R_{sigma} = 0.0387]
Data/restraints/parameters	3313/0/202
Goodness-of-fit on F^2	1.024
Final R indexes [I>=2σ (I)]	R_1 = 0.0371, wR_2 = 0.0845
Final R indexes [all data]	R_1 = 0.0587, wR_2 = 0.0943
Largest diff. peak/hole / e Å^{-3}	0.47/-0.55

Table S3. Crystal data and structure refinement for Ir complex **2b**.

Identification code	2b_sq
Empirical formula	$C_{21}H_{42}B_{10}Cl_2IrN_2$
Formula weight	693.76
Temperature/K	293(2)
Crystal system	hexagonal
Space group	$P6_1$
a/Å	35.0294(11)
b/Å	35.0294(11)
c/Å	13.0675(4)
α/°	90
β/°	90
γ/°	120
Volume/Å^3	13886.3(9)
Z	18
ρ_{calc}g/cm^3	1.493
μ/mm^{-1}	10.053
F(000)	6174.0
Crystal size/mm^3	0.24 × 0.03 × 0.02
Radiation	CuKα (λ = 1.54184)
2Θ range for data collection/°	5.826 to 108.33
Index ranges	-31 ≤ h ≤ 36, -36 ≤ k ≤ 24, -12 ≤ l ≤ 10
Reflections collected	25900
Independent reflections	9884 [R_{int} = 0.0622, R_{sigma} = 0.0756]
Data/restraints/parameters	9884/1288/910
Goodness-of-fit on F^2	1.070
Final R indexes [I>=2σ (I)]	R_1 = 0.0666, wR_2 = 0.1493
Final R indexes [all data]	R_1 = 0.0753, wR_2 = 0.1544
Largest diff. peak/hole / e Å^{-3}	1.10/-0.95
Flack parameter	-0.021(13)

Table S4. Crystal data and structure refinement for Ir complex **2c**.

Identification code	2c
Empirical formula	$C_{19}H_{37}B_{10}Cl_2IrN_2$
Formula weight	664.70
Temperature/K	120.0(2)
Crystal system	monoclinic
Space group	$P2_1/n$
a/Å	7.3551(4)
b/Å	15.9601(8)
c/Å	23.705(2)
α/°	90
β/°	92.623(6)
γ/°	90
Volume/Å^3	2779.8(3)
Z	4
ρ_{calc}g/cm^3	1.588
μ/mm^{-1}	11.134
F(000)	1304.0
Crystal size/mm^3	0.09 × 0.05 × 0.03
Radiation	CuKα (λ = 1.54184)
2Θ range for data collection/°	6.678 to 146.066
Index ranges	-8 ≤ h ≤ 8, -19 ≤ k ≤ 19, -26 ≤ l ≤ 29
Reflections collected	6983
Independent reflections	6983 [R_{int} = 0.070, R_{sigma} = 0.105]
Data/restraints/parameters	6983/447/315
Goodness-of-fit on F^2	1.098
Final R indexes [I>=2σ (I)]	R_1 = 0.0739, wR_2 = 0.1894
Final R indexes [all data]	R_1 = 0.1095, wR_2 = 0.2022
Largest diff. peak/hole / e Å^{-3}	2.91/-1.88

Table S5. Crystal data and structure refinement for Ir complex **2d**.

Identification code	2d
Empirical formula	$C_{22}H_{29}Cl_2IrN_2$
Formula weight	584.57
Temperature/K	120.01(10)
Crystal system	monoclinic
Space group	C2/c
a/Å	15.3524(4)
b/Å	8.7930(2)
c/Å	32.4934(11)
α/°	90
β/°	96.328(3)
γ/°	90
Volume/Å^3	4359.7(2)
Z	8
ρ_{calc}g/cm^3	1.781
μ/mm^{-1}	6.380
F(000)	2288.0
Crystal size/mm^3	0.29 × 0.18 × 0.11
Radiation	MoKα (λ = 0.71073)
2Θ range for data collection/°	6.038 to 62.436
Index ranges	-22 ≤ h ≤ 21, -12 ≤ k ≤ 11, -44 ≤ l ≤ 46
Reflections collected	15520
Independent reflections	6181 [R_{int} = 0.0501, R_{sigma} = 0.0667]
Data/restraints/parameters	6181/0/250
Goodness-of-fit on F^2	1.066
Final R indexes [I>=2σ (I)]	R_1 = 0.0435, wR_2 = 0.0929
Final R indexes [all data]	R_1 = 0.0567, wR_2 = 0.1015
Largest diff. peak/hole / e Å^{-3}	2.20/-1.88

Table S6. Crystal data and structure refinement for Ir complex **4a**.

Identification code	4a
Empirical formula	$C_{21}H_{39}B_{10}IrN_2$
Formula weight	619.84
Temperature/K	120.01(10)
Crystal system	monoclinic
Space group	$P2_1/n$
a/Å	11.1388(4)
b/Å	18.2073(6)
c/Å	13.5279(5)
α/°	90
β/°	110.343(4)
γ/°	90
Volume/Å^3	2572.45(18)
Z	4
ρ_{calc}g/cm^3	1.600
μ/mm^{-1}	5.205
F(000)	1224.0
Crystal size/mm^3	0.08 × 0.07 × 0.04
Radiation	MoKα (λ = 0.71073)
2Θ range for data collection/°	6.07 to 62.374
Index ranges	-14 ≤ h ≤ 16, -26 ≤ k ≤ 26, -19 ≤ l ≤ 19
Reflections collected	25348
Independent reflections	7490 [R_{int} = 0.0466, R_{sigma} = 0.0558]
Data/restraints/parameters	7490/0/314
Goodness-of-fit on F^2	1.024
Final R indexes [I>=2σ (I)]	R_1 = 0.0329, wR_2 = 0.0539
Final R indexes [all data]	R_1 = 0.0485, wR_2 = 0.0577
Largest diff. peak/hole / e Å^{-3}	1.03/-0.96

Table S7. Crystal data and structure refinement for Ru complex **6b**.

Identification code	6b
Empirical formula	$C_{18}H_{34}B_{10}Cl_2N_2Ru$
Formula weight	558.54
Temperature/K	119.99(12)
Crystal system	monoclinic
Space group	Ia
a/Å	11.8583(3)
b/Å	19.1551(4)
c/Å	12.2719(3)
α/°	90
β/°	112.782(3)
γ/°	90
Volume/Å^3	2570.05(13)
Z	4
ρ_{calc}g/cm^3	1.444
μ/mm^{-1}	6.907
F(000)	1136.0
Crystal size/mm^3	0.11 × 0.03 × 0.02
Radiation	CuKα (λ = 1.54184)
2Θ range for data collection/°	9.078 to 146.688
Index ranges	-11 ≤ h ≤ 14, -23 ≤ k ≤ 22, -14 ≤ l ≤ 15
Reflections collected	4773
Independent reflections	2923 [R_{int} = 0.0419, R_{sigma} = 0.0576]
Data/restraints/parameters	2923/38/302
Goodness-of-fit on F^2	1.088
Final R indexes [I>=2σ (I)]	R_1 = 0.0507, wR_2 = 0.1245
Final R indexes [all data]	R_1 = 0.0516, wR_2 = 0.1258
Largest diff. peak/hole / e Å^{-3}	1.91/-1.95
Flack parameter	-0.010(18)

Table S8. Crystal data and structure refinement for Ir complex **7b**.

Identification code	7b
Empirical formula	$C_{18}H_{34}B_{10}Br_{0.7}Cl_{0.3}IrN_2$
Formula weight	645.34
Temperature/K	120.0(2)
Crystal system	triclinic
Space group	P-1
a/Å	8.0693(4)
b/Å	10.6249(4)
c/Å	14.7046(7)
α/°	95.466(4)
β/°	93.488(4)
γ/°	106.566(4)
Volume/Å^3	1197.76(10)
Z	2
ρ_{calc}g/cm^3	1.789
μ/mm^{-1}	6.786
F(000)	625.0
Crystal size/mm^3	0.28 × 0.17 × 0.08
Radiation	MoKα (λ = 0.71073)
2Θ range for data collection/°	6.282 to 62.672
Index ranges	-11 ≤ h ≤ 11, -12 ≤ k ≤ 14, -17 ≤ l ≤ 21
Reflections collected	14195
Independent reflections	6744 [R_{int} = 0.0436, R_{sigma} = 0.0766]
Data/restraints/parameters	6744/0/295
Goodness-of-fit on F^2	1.002
Final R indexes [I>=2σ (I)]	R_1 = 0.0468, wR_2 = 0.0942
Final R indexes [all data]	R_1 = 0.0610, wR_2 = 0.1005
Largest diff. peak/hole / e Å^{-3}	4.07/-1.78

References

1. G. M. Sheldrick, Acta. Crystallogr. A, 2008, 64, 112-122.
2. G. M. Sheldrick, Acta Crystallogr. A, 2015, 71, 3-8.
3. G. M. Sheldrick, Acta Crystallogr. C, 2015, 71, 3-8.
4. O. V. Dolomanov, L. J. Bourhis, R. J. Gildea, J. A. K. Howard and H. Puschmann, J. Appl. Cryst., 2009, 42, 339-341.
5. Persistence of Vision Pty. Ltd. (2004), Persistence of Vision Raytracer (Version 3.7)
6. L. J. Barbour, J. Supra. Chem., 2001, 1, 189-191.